AN ANALYTICALLY LINEARIZED HELICOPTER MODEL WITH IMPROVED MODELING ACCURACY

by

Patrick T. Jensen
H. C. Curtiss, Jr.

Princeton University
Department of Mechanical and Aerospace Engineering
Princeton, NJ 08544-5263

INTERIM REPORT
(August 1, 1990 - August 1, 1991)

NASA Ames Grant No. NAG 2-561
Studies in Rotorcraft Systems Identification

Principle Investigators

H. C. Curtiss, Jr.
R. M. McKillip, Jr.

August 1991

TABLE OF CONTENTS

ACKNOWLEDGEMENTS ii

LIST OF ILLUSTRATIONS v

LIST OF TABLES viii

NOTATION ix

ABSTRACT xiii

Chapter

I. INTRODUCTION 1

II. THE ANALYTICALLY LINEARIZED HELICOPTER MODEL. . 6

2.1 Generation of the Model 6
2.2 The Lagrangian Formulation 8
2.3 Linearization of the System 13
2.4 State-Space Representation 15
2.5 The Quasi-Static Formulation 17
2.6 Dynamic Inflow Modeling 20
2.7 Rotor Wake Effects on the Tail 22
2.8 Benefits of Analytic Linearization and the Trim Input File 23

III. VALIDATION OF THE MODEL WITH FLIGHT TEST . . . 25

3.1 The UH-60A Black Hawk Helicopter 25
3.2 USAAEFA Flight Test 30
3.3 Prior Validation of Other Simulation Models . . . 33
3.4 Flight Test Correlation of the Original Analytically Linearized Model 34

IV. MODEL IMPLEMENTATION IMPROVEMENTS 39

V. HELICOPTER MODEL IMPROVEMENTS 43

5.1 Rotor Forces Resolved to the Body 43
5.2 Trim Force and Moment Corrections 47
5.3 Rotor Inertia Velocity Terms 54
5.4 Style Improvements 54

VI. TRIM INPUT FILE FOR THE SYSTEM 56

6.1 Stabilator Incidence Angle 56
6.2 Linear Geometric Twist 58
6.3 Control System Input Phase Angle 60
6.4 Steady-State Coning and Lag Angles 61
6.5 Main Rotor and Tail Rotor Pitch 63
6.6 Uniform Induced Velocity 64
6.7 Other Corrections 65

VII. RESULTS OF THE CHANGES 66

VI. CONCLUSIONS AND RECOMMENDATIONS. 74

REFERENCES 76

LIST OF ILLUSTRATIONS

Figure		Page
2-1	Rotor flap degrees of freedom.	8
2-2	Rotor lag degrees of freedom.	9
2-3	Hub and fuselage axis systems	10
2-4	Lateral and longitudinal cyclic input to the rotor	12
2-5	Roll response of the 24 state model, without dynamic inflow effects, to a 1" lateral cyclic input in a hover (AEFA Test 201)	17
2-6	Roll response of the 12 state model , with dynamic inflow effects, to a 1" lateral cyclic input in a hover (AEFA Test 201)	19
2-7	Dynamic inflow components	20
2-8	Roll response of the full 27 state model, with dynamic inflow effects, to a 1" lateral cyclic input in a hover (AEFA Test 201)	22
3-1	UH-60A Black Hawk helicopter	26
3-2	UH-60A control system logic, illustrating the control mixing	28
3-3	Roll rate response of the original 27 state model, with dynamic inflow effects, to a 1" right cyclic input, in a hover (AEFA Test 201)	35
3-4	Pitch rate response of the original 27 state model, with dynamic inflow effects, to a 1" right cyclic input, in a hover (AEFA Test 201)	35
3-5	Yaw rate response of the original 27 state model, with dynamic inflow effects, to a 1" right cyclic input, in a hover (AEFA Test 201)	36

3-6 Roll rate response of the original 27 state model, with dynamic inflow effects, to a 1/2" left then right doublet pedal input, at 140 knots (AEFA Test 309) . . . 36

3-7 Pitch rate response of the original 27 state model, with dynamic inflow effects, to a 1/2" left then right doublet pedal input, at 140 knots (AEFA Test 309) . . . 37

3-8 Yaw rate response of the original 27 state model, with dynamic inflow effects, to a 1/2" left then right doublet pedal input, at 140 knots (AEFA Test 309) . . . 37

4-1 Original implementation of the model 40

4-2 Improved implementation of the model 41

5-1 Definition of the waterline/frame-station/butt-line reference system 44

5-2 Hub and fuselage c.m. geometry 44

5-3 Geometry for a shaft tilted by the angle AN 46

5-4 Calculated forces and moments on the blade and hub . . . 48

5-5 Body, shaft, and control axis angles of attack 51

5-6 Blade pitch angle for trim flight at 140 knots (AEFA Test 309) 52

6-1 Geometric blade twist for the actual and modeled blade . . 59

6-2 Control system input phase angle, Δsp 61

6-3 Forces generating coning and lag 62

7-1 Response of the corrected full 27 state model, with dynamic inflow effects, to a 1" right cyclic input in a hover (AEFA Test 201) 67

7-2 Response of the corrected full 27 state model, with dynamic inflow effects, to a 1" left pedal input in a hover (AEFA Test 209) 69

7-3 Response of the corrected full 27 state model, with dynamic inflow effects, to a 1" left cyclic input at 60 knots (AEFA Test 504 70

LIST OF TABLES

Table		Page
1.	Physical interpretation of the parts of the generalized matrices **C** and **K**	14
2.	Stabilator position settings for the four flight test aim airspeeds	32
3.	Outcome of initial trim calculations	49
4.	Outcome of corrected trim calculations	54

NOTATION

$\mathbf{A}$	Linear system matrix.
a_o	Blade coning angle.
a_1	Longitudinal flapping angle.
A_{1s}	Lateral cyclic control input.
AN	Main rotor shaft tilt angle.
$\mathbf{B}$	Linear control matrix.
b_1	Lateral flapping angle.
B_{1s}	Longitudinal cyclic control input.
$\mathbf{C}$	"Generalized" damping matrix.
c.g.	Center of gravity.
c.m.	Center of mass.
C_L	Coefficient of lift.
$C_{L\alpha}$	Lift slope, $\partial C_L/\partial\alpha$.
C_T	Coefficient of thrust.
$\mathbf{D_c}$, $\mathbf{DB_1}$, $\mathbf{DB_2}$, $\mathbf{DF}$	Coefficients of the dynamic inflow equation.
E	Hinge offset.
$\mathbf{F}$	"Generalized" forcing matrix.
h	Height of rotor hub above fuselage c.g.
H_s	Rotor longitudinal force resolved to the shaft.
$\mathbf{I}$	Identity matrix.
I_b	Blade moment of inertia.
I_{xx}	Aircraft roll moment of inertia.

I_{yy}	Aircraft pitch moment of inertia.
I_{zz}	Aircraft yaw moment of inertia.
K	"Generalized" spring matrix.
L	Unsteady aerodynamic effect matrix.
M	"Generalized" mass matrix.
m_b	Blade mass.
m_{fus}	Fuselage mass.
M_t, M_w, M_{cf}, M_i, M_d,M_{hs}	Blade moments due to thrust, weight, centrifugal force, inertia, drag, and hub springs, respectively.
Q	Generalized coordinate vector.
q	Perturbational generalized coordinate vector.
R	Main rotor radius.
r	Radial position on the blade.
S_b	Blade first moment.
T	Time.
T	Transformation matrix.
T_s	Rotor vertical force resolved to the shaft.
U	Generalized input vector.
u	Perturbational generalized input vector.
v	Induced velocity vector.
v_o	Uniform induced velocity.
X	Longitudinal axis.
x	State vector.
X_c	Collective position.
x_{cg}	Distance of the c.g. aft of the hub.
$\mathbf{X}_{hub}$	Vector of hub translational and angular position.

X_{LAT}	Cyclic lateral position.
X_{LONG}	Cyclic longitudinal position.
$\mathbf{X}_{shaft}$	Vector of shaft translational and angular position.
X_{TR}	Direction pedal position for the tail rotor input.
Y	Lateral axis.
Y_s	Rotor lateral force resolved to the shaft.
Z	Vertical axis.
0	Null vector.
α	Angle of attack.
α_2	Rotor pitch/lag coupling angle.
β	Blade flap angle.
δ_3	Rotor pitch/flap coupling angle.
Δsp	Control system input phase angle.
ϕ	Roll angle.
γ_1	Coefficient corresponding to the lateral displacement of the rotor c.m.
γ_2	Coefficient corresponding to the longitudinal displacement of the rotor c.m.
λ	Rotor inflow ratio.
μ	Tip speed ratio.
ν	Induced dynamic inflow.
ν_c	Longitudinal variation in dynamic inflow.
ν_o	Uniform dynamic inflow.
ν_s	Lateral variation in dynamic inflow.
θ	Pitch angle.
θ_o	Main rotor collective pitch angle.

θ_{TR}	Tail rotor collective pitch angle.
Ω	Rotor speed.
Ψ	Rotor azimuth angle.
ψ	Yaw angle.
ζ	Rotor lag angle.
ζ_0	Uniform lag angle.

Superscripts:

^{T}	Matrix transpose.
$^{-1}$	Matrix inverse.
$\dot{}$	First time derivative.
$\ddot{}$	Second time derivative

ABSTRACT

An analytically linearized model for helicopter flight response including rotor blade dynamics and dynamic inflow, that was recently developed, has been studied with the objective of increasing the understanding, the ease of use, and the accuracy of the model. The mathematical model is described along with a description of the UH-60A Black Hawk helicopter and flight test used to validate the model. To aid in utilization of the model for sensitivity analysis, a new, faster, and more efficient implementation of the model has been developed. It is shown that several errors in the mathematical modeling of the system have caused a reduction in accuracy. These errors in rotor force resolution, trim force and moment calculation, and rotor inertia terms have been corrected along with improvements to the programming style and documentation. Use of a trim input file to drive the model is examined. Trim file errors in blade twist, control input phase angle, coning and lag angles, main and tail rotor pitch, and uniform induced velocity, have been corrected. Finally, through direct comparison of the original and corrected model responses to flight test data, the effect of the corrections on overall model output is shown.

CHAPTER I

INTRODUCTION

Progress in helicopter technology requires progress in the ability to analyze those helicopters. In both the initial design phases and the modification phases of helicopter development, the engineer must be capable of accurately modeling his design to observe the behavior of its various components. The aeroelastic and aeromechanical stability and control response problems in helicopters are of particular interest and, unfortunately, tend to be among the most complicated problems faced by dynamicists. Studying the stability and control response of a helicopter presents the designer with a number of challenges that do not affect the designer of fixed wing aircraft. The interaction and coupling between the rotor system dynamics and the helicopter body dynamics presents a problem that is usually modeled by a system of complex nonlinear equations. Although there are several ways to handle these nonlinear equations, many are not adequately suitable for stability and control analyses and do not provide a physical insight into the problem. An analytically linearized model of the full dynamics of the nonlinear system, however, does have a great potential in this area. This research further examines, clarifies, and corrects a unique mathematical model [1] developed several years ago, that may be suitable for many of these types of analyses.

Historically, helicopter analysis has often been based on a quasi-static, rigid body stability derivative model in which the blade dynamics are

neglected. Rotor flap and lag angles are determined from the instantaneous values of body angular and translational displacements as well as body rates and accelerations. For many applications, such as low frequency response and steady state flight behavior, this approach is adequate and is sufficiently simple to promote a physical insight into the problem.

However, back in the early 1950's, there was doubt as to the capabilities of the quasi-static model. Ellis [2] found that due to the neglecting of the strong influence of the rotor dynamics, the conventional quasi-static stability derivative model was not capable of representing higher order, short period dynamics. More recent studies by Hansen [3] found that the flapping dynamics, which are neglected in the quasi-static model, were very important in stability derivative determination.

It has also been determined that the quasi-static model may not be adequate for the development of feedback control systems. Curtiss [4] found that the high frequency modes associated with the body-flap coupling and the lag degrees of freedom limited the rate and attitude feedback gains used in attitude control systems. This was not predicted by the quasi-static formulation. Hall [5] showed that, for tight control (high gain), neglecting the rotor flapping dynamics in the design of the feedback system resulted in unstable closed loop responses when the flap dynamics were included. Zhao [1] discovered that the lag dynamics, as well, caused instability in the closed loop response if they were neglected in the design of the feedback control system.

Additionally, several researchers (Curtiss and Shupe [6], Gaonkar [7], and Chen [8]) determined that inclusion of dynamic inflow is important in modeling the helicopter. The dynamic inflow was found to produce

significant changes in the response modes due to the influence of the low frequency unsteady aerodynamics.

The shortcomings of the quasi-static formulation for stability and control analysis becomes even more severe as helicopter technology progresses. Super augmented, high-gain flight control systems are being developed for military helicopters in order to meet the requirements of demanding mission tasks such as low level, nap-of-the-earth flight. The rotor designs are shifting to more hingeless and bearingless systems which tend to be more prone to rotor-fuselage mechanical instabilities. In addition, the fly-by-wire and fly-by-light control systems being developed are so fast and so responsive that the modeling of rotor blade dynamics becomes an essential component of the modeling process. The obvious conclusion is that the true physical behavior of the highly coupled rotor-fuselage dynamical system can only be fully captured by developing a model in which the influence of the coupled rotor-body motion is properly incorporated and for which the effects of unsteady aerodynamics are accounted.

One solution to deal with these problems results in a system consisting of nonlinear ordinary differential equations with periodic coefficients. Sikorsky's GENHEL [9] is an example of such a nonlinear program. Although this model can provide a reasonable simulation of the dynamic response of the helicopter to time varying inputs, the complication level is so high that gaining a general understanding of the system or a physical insight into the problem is very difficult, if not impossible.

An excellent alternative solution would be a carefully linearized description of the nonlinear equations about a steady-state trim condition. This would provide for analytical simplicity and could be used as a basis for

the design of feedback control systems. This linearized system would be especially attractive if it could be shown to agree with experiment.

Recently, a linearized model was developed by Zhao [1] as part of his doctoral research in Aerospace Engineering at Princeton University. The generic model, which is capable of representing any single main rotor helicopter, uses an analytically linearized form of the equations, incorporating rotor dynamics and dynamic inflow effects. This provides for the accurate representation required for the stability and control analysis of a helicopter. To ensure that the model was properly representing true aircraft response, it was compared to flight test data. The simulation showed very good agreement with a UH-60A Black Hawk helicopter for both hover and forward flight speeds. This particular aircraft was used for the validation because high quality flight test data were readily available [10]. MacDonald performed further research [11] on this generic model with the goal of improving the correlation of Zhao's model to flight test data through the correction of modeling errors and application of an analytical study.

The present research continues the development and improvement of this generic linearized model with several overall objectives. The full system model, the quasi-static simplified version, and the incorporation of dynamic inflow terms is clarified and documented to aid in further research and development of the program. The UH-60A Black Hawk flight test data are clarified and described with an emphasis on subtleties or irregularities that impact simulation of the flight conditions. Also, the user interface is improved in order to facilitate expedient sensitivity analysis used in the further development of the model. The main thrust of this research, however is to correct modeling errors in order to improve the accuracy of the

model and to improve the understanding of the inputs required to drive the simulation. This last part is accomplished through sensitivity analyses of the model response to variations in selected parameters.

CHAPTER II

THE ANALYTICALLY LINEARIZED HELICOPTER MODEL

2.1 Generation of the Model

The mathematical model created by Zhao [1] develops equations of motion based on a representation of a helicopter that includes a fuselage, an empennage consisting of a vertical tail, a horizontal tail, and a tail rotor, and a main rotor system maintained at a constant speed that consists of one hub and a number of blades associated with that hub.

Each blade is assumed to be a rigid beam that undergoes flap (vertical) and lag (inplane) bending. Torsional bending, however, is not included. The aerodynamic load on the blades is modeled using quasi-steady strip theory. The rotor hub is modeled as an articulated system with offset hinges, but the flexibility of the model allows other hub types, such as a hingeless or bearingless hub, to be modeled by the inclusion of the proper combination of a hinge offset and flap and lag springs. In addition, longitudinal tilt of the rotor shaft, pitch changes due to fuselage deformation, and the effects of a δ_3 or a α_2 hinge can be taken into account. Dynamic stall and reverse flow effects are not modeled. A simplified model of the tail rotor allows for coning of the blades but not for cyclic flap. It also allows for incorporation of a δ_3 hinge and a canted tail rotor shaft.

In order to properly couple the rotor with the rest of the helicopter, the equations for each blade are first developed in a coordinate system that rotates with the hub at a constant speed. These equations in the rotating coordinate

system are then transformed to the non-rotating system to be combined with the other blades and with the fuselage. Although this is actually just a transformation of coordinate systems, the mathematics involved can become quite lengthy and prone to algebraic errors.

Fortunately, the development of symbolic computer languages for general computer systems allows the development of the system dynamic equations directly on the computer. Zhao utilized a symbolic generation system called REDUCE, running on an IBM mainframe computer at the Princeton University Computing Center to develop the equations for the model. An added benefit of the REDUCE system was its ability to output the equations in program-ready FORTRAN code, again avoiding a source of errors. The equations were then checked with the symbolic system MACSYMA at the Laboratory for Control and Automation at Princeton.

Finally, the complete nonlinear dynamic description of the multi-dimensional system, formulated by a Lagrangian approach, is converted to a set of linear second-order differential equations. This is accomplished through a perturbation analysis performed on the nonlinear equations, and is described later in this chapter.

One of the greatest strengths of this model is the fact that by using symbolic manipulation, the final linear equations are strictly analytical and not numerical. Thus, the equations are applicable to any single main rotor helicopter in any trim flight condition without further modification. This allows a great flexibility in using the equations to study various helicopters and flight conditions by simply changing the values in a trim input file. Additionally, studies of the sensitivity of the helicopter (or the model) to slightly differing trim conditions can be quickly and easily performed.

2.2 The Lagrangian Formulation

A Lagrangian formulation is based on a set of generalized coordinates that correspond to the degrees of freedom of the system. For this particular helicopter model, the appropriate number is twelve: six degrees of freedom for the rotor system and six degrees of freedom for the fuselage.

Each blade has one flap and one lag degree of freedom. However, when converting from the rotating frame to the fixed frame through the use of multi-blade coordinates, six degrees of freedom result; three flap and three lag degrees. Figure 2-1 graphically defines the flap degrees of freedom. These

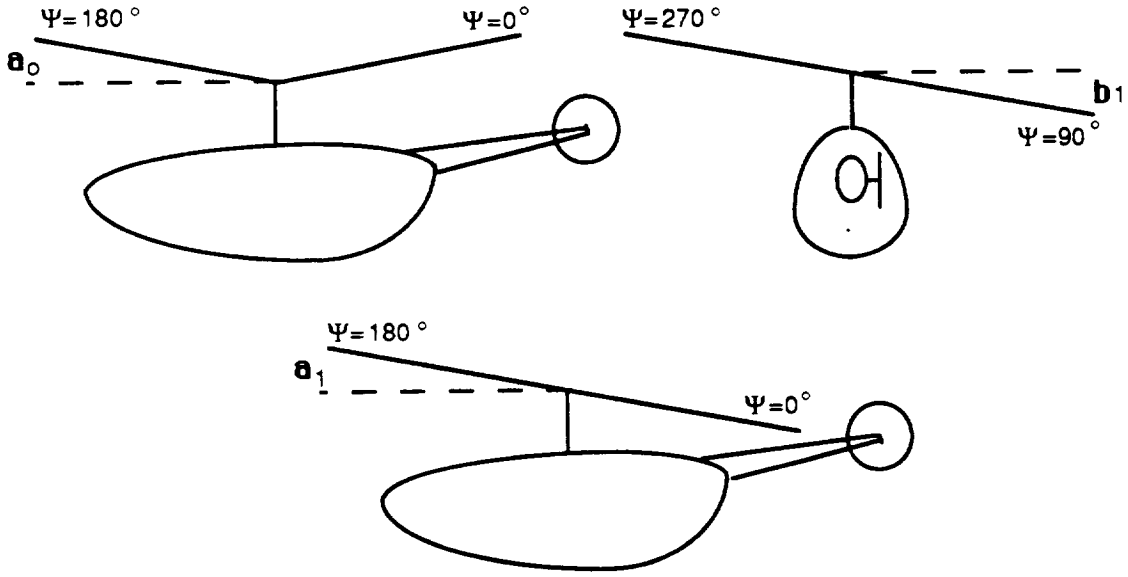

Figure 2-1: Rotor flap degrees of freedom.

three values correspond to the standard formulation for the flapping equation (NACA notation) as found in the literature [12],

$$\beta = a_0 - a_1 \cos(\Psi) - b_1 \sin(\Psi). \qquad (2.2\text{–}1)$$

β is the total flap angle, positive in the upward direction. a_0 is the part of the

flapping angle that is independent of blade azimuth angle Ψ. It is also positive in the upward direction. The coefficient a_1 represents the amplitude of a pure cosine motion for longitudinal tilt, positive for a flap back, and b_1 represents the amplitude of a pure sine motion for lateral tilt, positive for a flap down to the right.

In a similar manner, the three lag degrees of freedom are graphically defined in figure 2-2. Again these values correspond to a standard

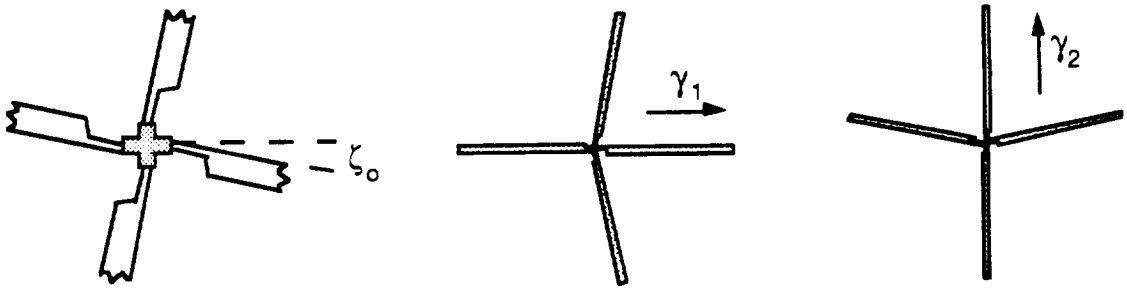

Figure 2-2: Rotor lag degrees of freedom.

formulation for the lag equation,

$$\zeta = \zeta_o - \gamma_1 \cos(\Psi) - \gamma_2 \sin(\Psi). \qquad (2.2\text{–}2)$$

ζ is the lag angle, positive for lag (motion opposite to rotation). ζ_o is the steady state lag which is positive in the same direction. The coefficient γ_1 corresponds to the lateral displacement of the center of mass (c.m.) of the rotor system due to asymmetric lag, positive to the right. Finally, γ_2 corresponds to the longitudinal displacement of the rotor system c.m., positive forward.

Six degrees of freedom are associated with the fuselage as well. There are three translational displacements in the lateral, longitudinal and vertical

direction. There are also three rotations in pitch, roll, and yaw. Due to a somewhat unconventional axis system used in the derivation of the model, the body forces and moments do not all follow the same sign conventions as the rotor system forces and moments. Figure 2-3 depicts the axes and positive sense of rotation for both systems. The X forward, Y right and Z down system that is usually encountered in stability and control analysis has not been used. An axis system similar to what is used in analyzing a rotor is used instead. Therefore, for both the hub and fuselage the Z axis is positive up, the Y axis is positive to the right, and the X axis is positive aft.

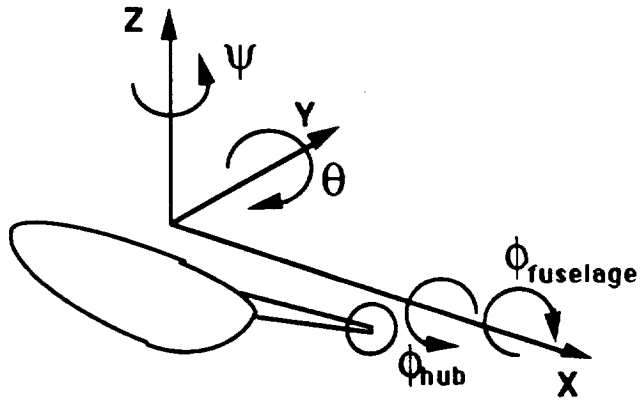

Figure 2-3: Hub and fuselage axis systems.

This unconventional axis system creates confusion in the definition of the rotations. Pitch, θ, remains positive in the nose up direction as per convention. Roll, ϕ, and yaw, ψ, are opposite of convention leading to a roll that is positive left wing down, and a yaw that is positive nose left. To relieve some of this confusion, the definition of the fuselage roll angle is reversed to positive right wing down, per convention, but the yaw remains unconventional throughout the program and is corrected only in the final

integration and plotting of the output. This change of sign for the roll angle does help in relieving some confusion, but it adds the side-effect of creating a left-handed system for the fuselage calculations. This can create problems in the definition of terms like products of inertia so careful consideration must be taken. Care must also be taken in transmitting rolling motion from the rotor system to the fuselage.

These six rotor degrees of freedom and the six fuselage degrees of freedom makeup the twelve generalized coordinates for the Lagrangian formulation. They are collected into a single vector, $\mathbf{Q}$,

$$\mathbf{Q} = [\, a_0, a_1, b_1, \zeta_0, \gamma_1, \gamma_2, \theta, \phi, \psi, y, x, z \,]^T. \tag{2.2-3}$$

Typical flight controls used by the helicopter pilot (collective stick, cyclic stick, and directional pedals) create three inputs to the main rotor system and one to the tail rotor. For the main rotor, they are the collective pitch of all the blades θ_0, the longitudinal cyclic pitch of the blades B_{1s}, and the lateral cyclic pitch of the blades A_{1s}. As with the flap and lag equations, the blade pitch (feathering) variables used in this program are in standard NACA notation,

$$\theta = \theta_0 - A_{1s} \cos(\Psi) - B_{1s} \sin(\Psi). \tag{2.2-4}$$

As shown in figure 2-4, the lateral cyclic pitch, A_{1s}, is positive right side down with the blade pitch at its most negative angle over the tail ($\Psi = 0°$). The longitudinal cyclic pitch, B_{1s} is positive nose down with the blade pitch at its most positive angle at $\Psi = 270°$. The input to the tail rotor is the value of collective pitch, θ_{TR}.

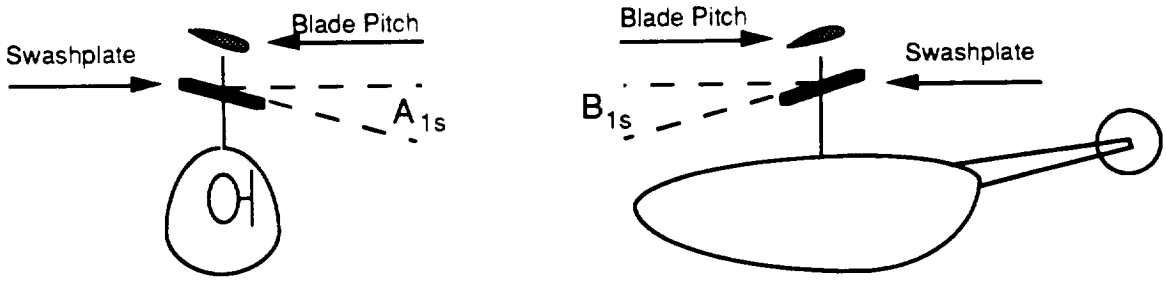

Figure 2-4: Lateral and longitudinal cyclic input to the rotor.

This model was originally designed for hover and level forward flight. In these cases, the value of collective pitch to the main rotor is not varied from a steady state trim value. Therefore, the constant trim value of θ_0 is provided to the model in the trim input file, and the system needs only three time varying inputs: the lateral cyclic pitch, the longitudinal cyclic pitch, and the tail rotor collective pitch. These values are contained in a vector of inputs, **U**,

$$\mathbf{U} = [\, A_{1s}, B_{1s}, \theta_{TR} \,]^T. \tag{2.2-5}$$

With the generalized coordinates and inputs defined, the nonlinear equations of motion can be developed using the Lagrangian approach. This results in a series of equations where the second time derivative of each generalized coordinate is expressed as a function of the first time derivative of the generalized coordinates, the generalized coordinates themselves, the inputs and time,

$$\ddot{\mathbf{Q}} = \mathbf{F}(\dot{\mathbf{Q}}, \mathbf{Q}, \mathbf{U}, T). \tag{2.2-6}$$

However, while introducing the multi-blade coordinates, which transformed

the rotating rotor system to the non-rotating frame, if the higher harmonic terms are omitted, a constant coefficient approximation to equation 2.2-6 is obtained,

$$\ddot{\mathbf{Q}} = F(\dot{\mathbf{Q}}, \mathbf{Q}, \mathbf{U}). \tag{2.2-7}$$

This is still a nonlinear representation of the Lagrangian formulated system, but it has constant coefficients.

2.3 Linearization of the System

This nonlinear system is then linearized using a perturbation analysis. In this sense, one assumes the twelve generalized coordinates, $\mathbf{Q}_i(t)$, and the three inputs, $\mathbf{U}_i(t)$, can be defined as the sum of a steady state value ($\mathbf{Q}_{io}$ or $\mathbf{U}_{io}$) and a time dependent perturbation around that steady state value ($\Delta\mathbf{Q}_i(t)$ or $\Delta\mathbf{U}_i(t)$),

$$\mathbf{Q}_i(t) = \mathbf{Q}_{io} + \Delta\mathbf{Q}_i(t), \tag{2.3-1}$$

$$\mathbf{U}_i(t) = \mathbf{U}_{io} + \Delta\mathbf{U}_i(t). \tag{2.3-2}$$

These new steady state plus perturbation terms are substituted into equation 2.2-7. Since the perturbation values are considered small (<<1), all terms containing squares of perturbation values are neglected. The perturbation quantities are then temporarily set equal to zero to obtain the steady-state values of the generalized coordinates and inputs. Since these steady-state values do not cause changes in the motion of the aircraft (by definition) they can be subtracted out. This leaves a second order, linear dynamic equation of motion for the helicopter,

$$M(Q_o,U_o)\,\Delta\ddot{Q} + C(Q_o,U_o)\,\Delta\dot{Q} + K(Q_o,U_o)\,\Delta Q = F(Q_o,U_o)\,\Delta U \qquad (2.3\text{-}3)$$

where **M** is a "generalized mass" matrix, **C** is a "generalized damping" matrix, **K** is a "generalized spring" matrix and **F** is the "forcing" matrix. Each is dependent on the constant, steady-state trim values of Q_o and U_o and are therefore constant matrices.

Due to the linearization of the system, these generalized matrices (**C**, **K** and **F**) can be treated as the superposition of the effects from individual components of the model as they are affected by the perturbations. This systematic modular approach permits the effects of any changes to the model to be observed directly on the system matrices. Table 1 indicates the physical interpretation of the parts of the **C** and **K** matrices. The total value of the matrix is the superposition (summation) of each term (i.e. **K**=**K**1+**K**2+...).

Table 1: Physical interpretation of the parts of the generalized matrices C and K.

C1 = Mechanical Damping	**K1** = Mechanical Spring
C2 = Aerodynamic Damping	**K2** = Aerodynamic Spring
C3 = (not used)	**K3** = Hinge and Elastic Coupling
C4 = Body Aerodynamic Damping	**K4** = Body Aerodynamic Spring
C5 = Vertical Tail Damping	**K5** = Vertical Tail Spring
C6 = Horizontal Tail Damping	**K6** = Horizontal Tail Spring
C7 = Tail Rotor Damping	**K7** = Tail Rotor Spring

The mass matrix, **M**, is treated slightly differently and contains the values of the inertias or masses required for the terms in the equations of motion. For example, the diagonal elements are basically the blade inertia (I_b) for the rotor degrees of freedom and the fuselage moments of inertia (I_{yy}, I_{xx}, and I_{zz}) or

the fuselage mass (m_{fus}) for the fuselage degrees of freedom. Other off-diagonal elements correspond similarly.

Because the values of the **M**, **C**, **K**, and **F** matrices are dependent on the trim condition ($\mathbf{Q}_o$,$\mathbf{U}_o$), it is important that the correct trim values are used in developing these matrices. There should not, however, be a strong dependence on the precise accuracy of the trim value. If a small change in one of the trim values makes a large change in the final output, then it would indicate difficulties with the linearization, and the validity of the model would have to be reviewed.

For clarity, equation 2.3-3 can be rewritten using a small letter **q** to represent the term $\Delta\mathbf{Q}$ and a small **u** to represent $\Delta\mathbf{U}$. This simplifies the equation to

$$\mathbf{M}\ddot{\mathbf{q}} + \mathbf{C}\dot{\mathbf{q}} + \mathbf{K}\mathbf{q} = \mathbf{F}\mathbf{u}. \tag{2.3-4}$$

Whereas the perturbations in generalized coordinates and inputs will be written $\mathbf{q} = [a_o,a_1,b_1,\zeta_o,\gamma_1,\gamma_2,\theta,\phi,\psi,y,x,z]^T$ and $\mathbf{u} = [A_{1s},B_{1s},\theta_{TR}]^T$, for the remainder of this report, it must be remembered that these are the values of the perturbation from the steady-state trim value, and not absolute values of the generalized coordinates or the absolute values of the inputs.

2.4 State-Space Representation

To further provide analytical simplicity, and to create a basis for development of feedback control systems, the system of second-order linear equations can be combined into a first order, state-space representation,

$$\dot{\mathbf{x}} = \mathbf{A}\mathbf{x} + \mathbf{B}\mathbf{u}. \tag{2.4-1}$$

This change is accomplished by noting the identity $\dot{\mathbf{q}} = \dot{\mathbf{q}}$, and manipulating equation 2.3-4 to read,

$$\dot{\mathbf{q}} = \dot{\mathbf{q}} \tag{2.4-2a}$$

$$\ddot{\mathbf{q}} = -\mathbf{M}^{-1}\mathbf{K}\mathbf{q} - \mathbf{M}^{-1}\mathbf{C}\dot{\mathbf{q}} + \mathbf{M}^{-1}\mathbf{F}\mathbf{u}. \tag{2.4-2b}$$

Then substituting $\mathbf{x} = [\,\mathbf{q},\ \dot{\mathbf{q}}\,]^T$, maintaining $\mathbf{u} = [A_{1s}, B_{1s}, \theta_{TR}]^T$, and writing in matrix form, the state-space representation is defined,

$$\dot{\mathbf{x}} = \begin{bmatrix} 0 & I \\ -M^{-1}K & -M^{-1}C \end{bmatrix}\mathbf{x} + \begin{bmatrix} 0 \\ M^{-1}F \end{bmatrix}\mathbf{u} \tag{2.4-3}$$

This conversion results in a state vector, $\mathbf{x}$, that consists of 24 states: the perturbations in the twelve generalized coordinates and their first time derivatives. This state-space form of the linearized model can now be conveniently used for eigenvalue analysis of the system (the eigenvalues of the matrix $\mathbf{A}$) or for integration over time with a specified, time varying input $\mathbf{u}$.

As an example, figure 2-5 shows the integration of equation 2.4-3 for a flight test input as calculated by MacDonald [11]. This graph of roll rate, which is a response to a one inch right lateral cyclic input in a hover, plots both the flight test roll rate and the basic simulation model output. The effects of dynamic inflow are not accounted for at this point. The model obviously reproduces the general shape of the aircraft response, although a large discrepancy in the maximum value is evident.

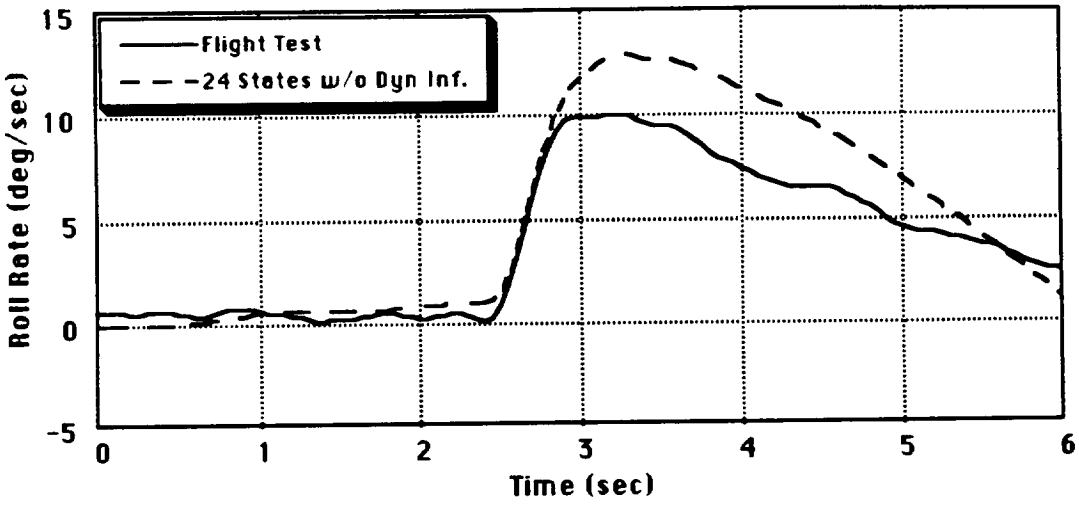

Figure 2-5: Roll response of the 24 state model, without dynamic inflow effects, to a 1" lateral cyclic input in a hover (AEFA Test 201).

2.5 The Quasi-Static Formulation

As discussed earlier, a quasi-static formulation that neglects the rotor dynamics is not capable of modeling the higher order, short period dynamics and can therefore cause instabilities in feedback control laws that may be developed. However, the quasi-static solution developed from a full order model does retain many of the important characteristics of the full system transient response. By having a reduced order (from 24 to 12), it also provides a reduction in the complexity of the model and a subsequent improvement in the physical insight that can be gained. This is especially evident when the quasi-static system response can be compared to the full order response.

MacDonald developed a quasi-static formulation from the full order model that provides these benefits. The simplified model is developed by noting that the rotor system response is much faster than the fuselage response. The assumption is made, therefore, that in terms of the time frame of the fuselage, an input to the rotor system causes the rotor to achieve its

new equilibrium position instantaneously.

Mathematically, this is achieved by first splitting the twelve generalized coordinates into two vectors: the body degrees of freedom, $\mathbf{q}_b$, and the rotor degrees of freedom, $\mathbf{q}_r$,

$$\mathbf{q}_b = [\, \theta, \phi, \psi, y, x, z \,]^T \quad \text{and} \quad \mathbf{q}_r = [\, a_o, a_1, b_1, \zeta_o, \gamma_1, \gamma_2 \,]^T . \tag{2.5-1}$$

The **M**, **C**, **K**, and **F** matrices can then be partitioned, and the equations of motion rewritten as

$$\begin{bmatrix} \mathbf{M}_{11} & \mathbf{M}_{12} \\ \mathbf{M}_{21} & \mathbf{M}_{22} \end{bmatrix} \begin{bmatrix} \ddot{\mathbf{q}}_b \\ \ddot{\mathbf{q}}_r \end{bmatrix} + \begin{bmatrix} \mathbf{C}_{11} & \mathbf{C}_{12} \\ \mathbf{C}_{21} & \mathbf{C}_{22} \end{bmatrix} \begin{bmatrix} \dot{\mathbf{q}}_b \\ \dot{\mathbf{q}}_r \end{bmatrix} + \begin{bmatrix} \mathbf{K}_{11} & \mathbf{K}_{12} \\ \mathbf{K}_{21} & \mathbf{K}_{22} \end{bmatrix} \begin{bmatrix} \mathbf{q}_b \\ \mathbf{q}_r \end{bmatrix} = \begin{bmatrix} \mathbf{F}_1 \\ \mathbf{F}_2 \end{bmatrix} \mathbf{u} \tag{2.5-2}$$

Setting the rotor system partitions of the **M** and **C** matrices, $\mathbf{M}_{12}$, $\mathbf{M}_{22}$, $\mathbf{C}_{12}$, and $\mathbf{C}_{22}$ equal to zero and manipulating the results gives an algebraic equation for the rotor states,

$$\mathbf{q}_r = - \mathbf{M}_E \ddot{\mathbf{q}}_b - \mathbf{C}_E \dot{\mathbf{q}}_b - \mathbf{K}_E \mathbf{q}_b + \mathbf{F}_E \mathbf{u} \tag{2.5-3}$$

where the subscript E denotes the effective matrices as computed in terms of the partitioned matrices of equation 2.5-2. Finally, setting $\ddot{\mathbf{q}}_r$ and $\dot{\mathbf{q}}_r$ equal to zero, since we are assuming that the change in $\mathbf{q}_r$ is instantaneous, and substituting equation 2.5-3 back into 2.5-2 we are able to write the quasi-static equations of motion in terms of a second order, linear equation in $\mathbf{q}_b$,

$$\mathbf{M}_Q \ddot{\mathbf{q}}_b + \mathbf{C}_Q \dot{\mathbf{q}}_b + \mathbf{K}_Q \mathbf{q}_b = \mathbf{F}_Q \mathbf{u}. \tag{2.5-4}$$

In the same manner as section 2.4, equation 2.5-4 can be converted into a convenient state space form. The resultant system is of order 12 (6 fuselage degrees of freedom and their first time derivatives), and this simplification

can aide in the understanding of the system response.

The response of the quasi-static model to the same right lateral input is shown in figure 2-6 along with the response of the 24 state model. In this case, the quasi-static response includes the effects of dynamic inflow as discussed in the next section. Although the overall roll rate response in this reduced order model is different from the basic full order model, the same initial roll acceleration is displayed. It is interesting to note that due to the

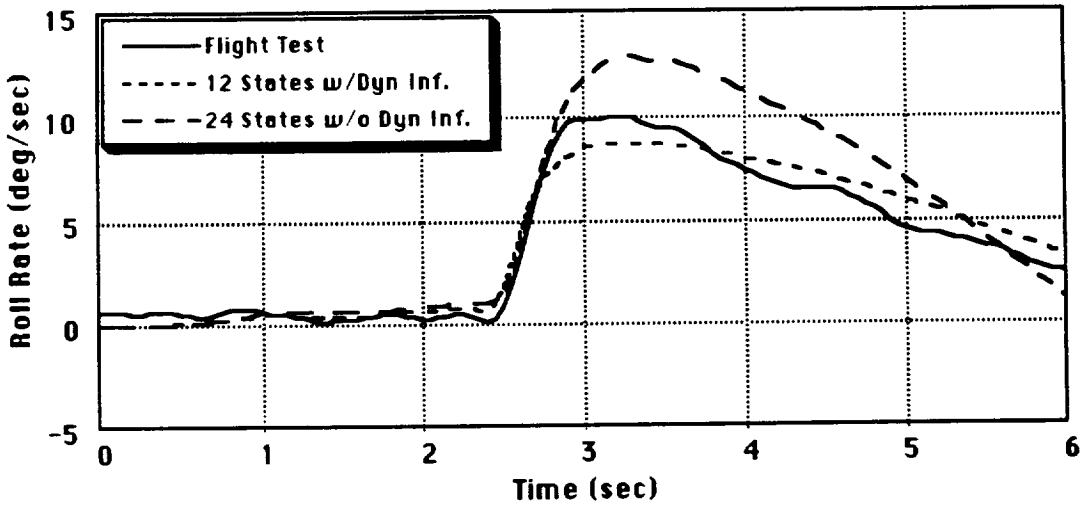

Figure 2-6: Roll response of the 12 state model, with dynamic inflow effects, to a 1" lateral cyclic input in a hover (AEFA Test 201).

"instantaneous" effects of the rotor system, the fuselage acceleration occurs slightly earlier than with the 24 state model. The lower peak indicates an increased roll damping as a side-effect of the reduction in model order and inclusion of the dynamic inflow effects. The smoothness of the model response curve is an indication of the lack of higher order rotor response modes which cause the slight oscillations noted in the flight test curve.

2.6 Dynamic Inflow Modeling

The unsteady aerodynamics of the rotor environment does have a significant impact on the response of the system so they need to be included in the model in order to accurately replicate the response of the aircraft. These aerodynamics can be modeled using simple models based on the definition of certain inflow parameters that represent the unsteady wake-induced flow through the rotor disk. As graphically defined in figure 2-7, these parameters include a steady state inflow, v_o, a cosine harmonic inflow coefficient, v_c , and a sine harmonic inflow coefficient, v_s. The harmonic

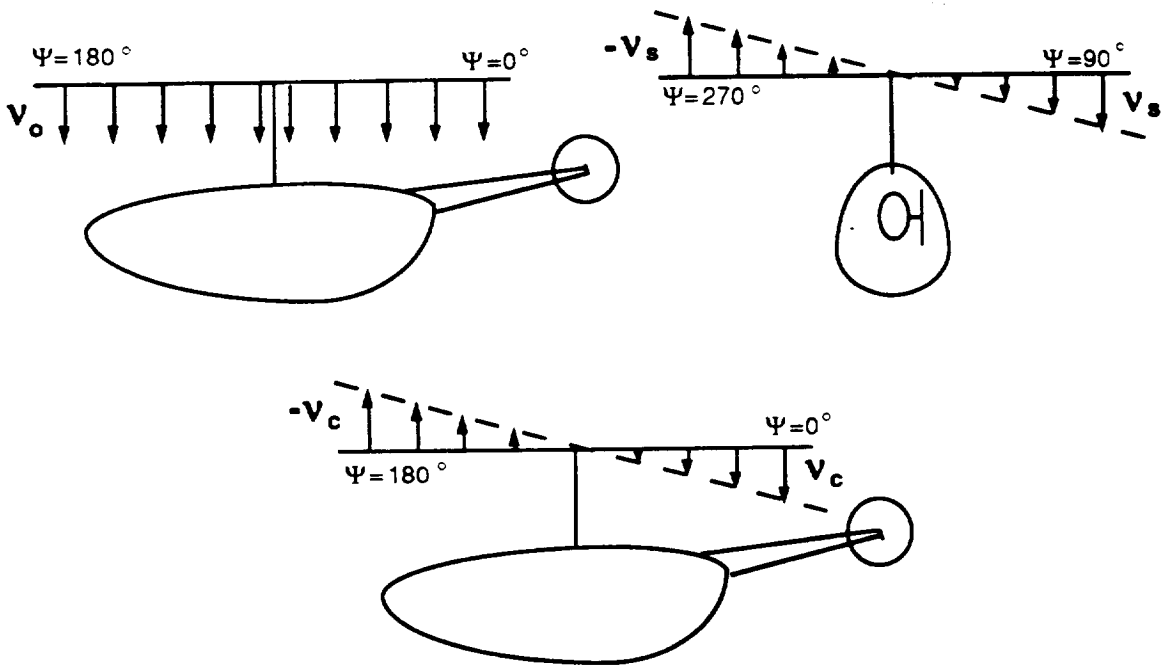

Figure 2-7: Dynamic inflow components.

components are assumed to vary linearly with radius, r. Mathematically, the total dynamic inflow is the sum of these terms,

$$\nu = \nu_0 + \nu_c\, r \cos(\Psi) + \nu_s\, r \sin(\Psi). \tag{2.6-1}$$

To model the dynamic inflow in the linearized equations of motion a term, **-Lv**, is added to account for the unsteady aerodynamics,

$$\mathbf{M}\ddot{\mathbf{q}} + \mathbf{C}\dot{\mathbf{q}} + \mathbf{K}\,\mathbf{q} - \mathbf{L}\,\mathbf{v} = \mathbf{F}\,\mathbf{u}. \tag{2.6-2}$$

v is the vector of the steady state inflow and the two harmonics. The dynamics of the inflow itself are included as an additional first order differential equation,

$$\dot{\mathbf{v}} = \mathbf{D_c}\,\mathbf{v} + \mathbf{DB_1}\,\mathbf{q} + \mathbf{DB_2}\,\dot{\mathbf{q}} + \mathbf{DF}\,\mathbf{u} \tag{2.6-3}$$

To convert the full order model with the dynamic inflow, to the state space representation, the same procedure is used as in section 2.4, but equation 2.6-3 is included with equations 2.4-2a and 2.4-2b in the formulation. This gives a slightly more complicated **A** and **B** matrix,

$$\mathbf{A}=\begin{bmatrix} \mathbf{0} & \mathbf{I} & \mathbf{0} \\ \mathbf{-M^{-1}K} & \mathbf{-M^{-1}C} & \mathbf{-L} \\ \mathbf{DB_1} & \mathbf{DB_2} & \mathbf{D_c} \end{bmatrix} \quad \text{and} \quad \mathbf{B}=\begin{bmatrix} \mathbf{0} \\ \mathbf{M^{-1}F} \\ \mathbf{DF} \end{bmatrix}, \tag{2.6-4}$$

for the augmented state variable, $\mathbf{x} = [\,\mathbf{q},\ \dot{\mathbf{q}},\ \mathbf{v}\,]^T$, which now is a vector of 27 states.

Inclusion of the unsteady aerodynamic effects into the full order model improves the response substantially. Figure 2-8 shows that the roll response of the model to the lateral cyclic input nearly coincides with the flight test data. The acceleration and damping have very good correlation with the flight test, and some higher order rotor mode oscillations are present. The response shows a great improvement over the 24 state or 12 state models.

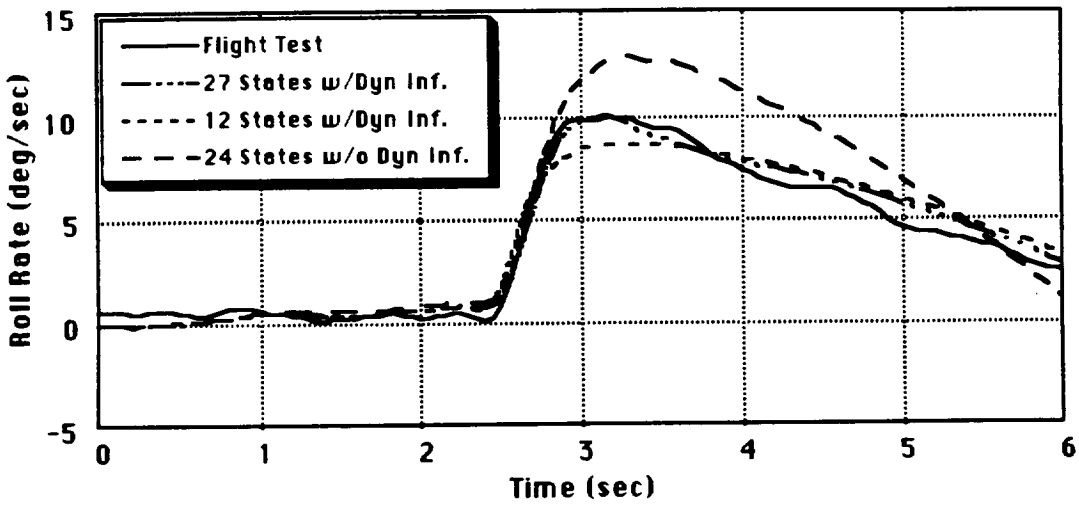

Figure 2-8: Roll response of the full 27 state model, with dynamic inflow effects, to a 1" lateral cyclic input in a hover (AEFA Test 201).

2.7 Rotor Wake Effects On The Tail

Wind tunnel tests have shown that the rotor wake has a large influence on the aerodynamics of the tail rotor and tail surfaces in forward flight. This influence arises from the variable downwash, sidewash, and forwardwash components of the rotor wake. Zhao, Curtiss and Quackenbush [13 & 14] found that modeling of helicopter transient response in forward flight is very sensitive to the treatment of the effects of the main rotor wake on the tail.

A vortex sheet, which is a continuous surface of vorticity, is formed by the vortices leaving the trailing edge of the main rotor blades. This vortex sheet forms the rotor wake. Application of the Biot-Savart law allows induced velocities to be calculated from this vortex sheet, and from these velocities, a rotor flow field can be developed. As the helicopter changes attitude, the angle of attack or sideslip will alter the position of the tail in this

flow field, thereby changing the aerodynamic forces and moments acting on the vertical tail, horizontal tail and tail rotor.

For this model, an off-line program is used to calculate these effects. Linearized derivatives are developed that model the change in the flow field with position. These values are then fed to the main program via the trim input file at the beginning of calculation and used to modify the system equations as necessary. The flexibility to input these wake effects, instead of having them coded in the main program, allows various simple or complicated models of the rotor wake to be used and compared.

2.8 Benefits Of Analytic Linearization and the Trim Input File

This model provides a unique basis to study sensitivities of the helicopter to variations in its parameters due to its having been analytically developed and linearized using the symbolic computer languages. It is this linearization that gives the model many advantages over other existing linearized models. These other models use numerical linearizations of the nonlinear equations about a set of flight conditions. Thus, the entire model, and not just the solution, would be fully dependent on the numerical value of the flight condition. It would not be possible to individually vary a single term of the nonlinear equation because these terms would be determined as part of the complete solution. For example, with the numerically linearized models, it would not be possible to change the steady state value of rotor coning in order observe the effect on the helicopter response or the eigenvalue analysis. The coning angle would be directly calculated from initial values of the flight condition (velocity, weight, air density, etc.) and would not be available to be changed directly by the dynamicist. The

analytically linearized model, however, does provide the ability to do this type of sensitivity analysis.

The model studied in this research uses a data file to input the required information to the mathematical model. This trim input file includes several types of information. One type is the physical dimensions of the helicopter such as main rotor diameter, blade twist, hinge offset distance, shaft tilt, vertical tail size and sweep, and tail rotor position. Additional physical characteristics that are input in the trim input file are data concerning the aerodynamics of the particular helicopter. These include main and tail rotor lift curve slopes, drag area, fuselage lift curve slope, and fuselage pitching moment slope. These values can be derived from fuselage wind tunnel data. Then the trim flight condition is input which includes values such as air density, weight, speed, and center of gravity (c.g.) position but also includes the trim values of main and tail rotor collective pitch, rotor speed, and body angle of attack. Much of this type of information comes directly from the flight test data. Other values, calculated off-line, are also included, like average induced flow for the tail and main rotors, wake effects on the tail surfaces, steady state rotor coning, and steady state blade lag.

Thus, modification of the trim input file allows the dynamicist to take full advantage of this analytically linearized model of the helicopter. Sensitivity of the aircraft (or the model) to the various parameters and conditions can be studied in isolation from other variations, and thereby greater insight and physical understanding can be gained.

CHAPTER III

VALIDATION OF THE MODEL WITH FLIGHT TEST

Any complex mathematical model of a dynamic system, especially one in which simplifying assumptions have been made, must be correlated with experiment to validate the accuracy of the model. To prove the validity of this analytically linearized model, it had to be correlated with actual helicopter responses.

In 1982 a flight test program was conducted with an early production UH-60A Black Hawk helicopter for the precise purpose of validating mathematical models [10]. The very high-quality step-input data that was developed in this study was used to validate other earlier simulation models of the Black Hawk. This data was made available to Princeton University and subsequently used to validate the linearized model studied in this research. Because the data had been correlated with other simulations, the added benefit of comparison with other mathematical models was available.

3.1 The UH-60A Black Hawk Helicopter

The UH-60A Black Hawk is a utility helicopter developed by Sikorsky for the Army under the Utility Tactical Transport Aircraft System (UTTAS) program. This medium sized helicopter is designed to carry 11 combat equipped troops and a crew of three. The twin-engine aircraft has a single main rotor and a canted tail rotor. A moveable horizontal stabilator is located on the lower portion of the tail pylon near the non-retractable tail wheel.

There are also two non-retractable main landing wheels mounted forward on the fuselage. Figure 3-1 shows the general external configuration of the Black Hawk helicopter. Further information on the helicopter structural and aerodynamic properties are given in reference [15].

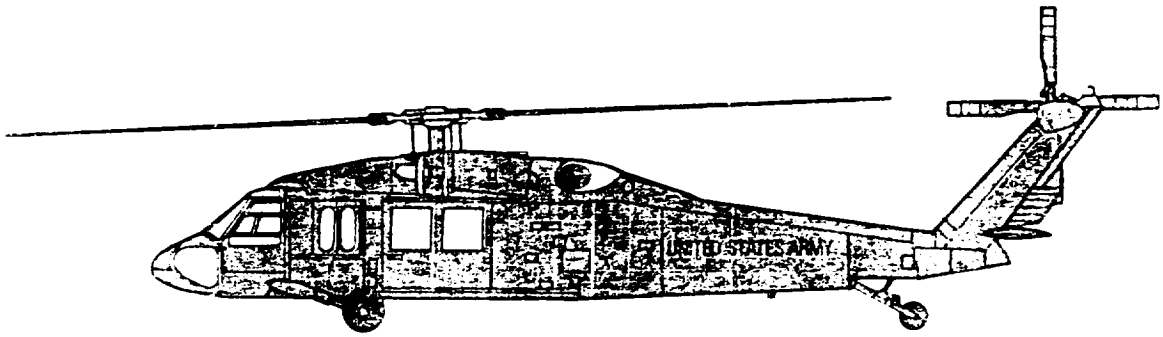

Figure 3-1: UH-60A Black Hawk helicopter.

The main rotor consists of four fully-articulated titanium/fiberglass blades which are retained by a flexible elastomeric bearing in a forged titanium hub. The elastomeric bearing, located at an offset of 1.25 feet from the shaft center, provides for pitch change as well as serving as the hinge for blade flap and lag. A conventional hydraulic damper acts to increase lag damping.

The cross-beam tail rotor with composite blades is attached to the right side of the tail pylon. It is a bearingless arrangement allowing for blade bending and pitch change solely through the flexibility built into the composite material of the blades. In addition, there is a 35 degree δ_3 hinge built into the blades that allows for a decrease in blade pitch with an increase in coning. This acts to reduce the blade flapping that occurs as a function of speed. The tail rotor is canted 20 degrees to provide 2.5 percent of total aircraft

lift in a hover, which also allows for greater aft center of gravity (c.g.) travel. An adverse side-effect of the canted tail rotor is that it adds additional coupling between the longitudinal and lateral motions of the aircraft.

To partially compensate for this coupling and to convert control stick motion into rotor inputs, the flight controls are fed through a "mixing unit." This mechanical device, made up of levers, cams and pushrods, has the expressed purpose of combining and coupling the cyclic, collective, and yaw inputs and providing proportional output to the main and tail rotor controls. However, it is also designed to de-couple some of the adverse affects of the canted tail rotor. It is important to note that the mixing unit is a mechanical system that has been designed for a certain "typical" flight condition. Therefore, at any other flight conditions, it will not operate optimally and may even produce some adverse side-effects of its own. These effects are minor but do show up in flight test responses and therefore should be expected in the simulation responses.

To illustrate the control mixing, the control system logic is shown in figure 3-2. In addition to the conversion from a control position to its corresponding input, as shown in the four bold boxes in figure 3-2, the other mixing is also presented. Collective stick position is fed-forward to the tail rotor pitch to counter the increased torque of a higher collective setting. Collective stick position is also fed to the lateral cyclic pitch, A_{1s}, to account for the increased thrust of the tail rotor from the previously described mixing. This increased tail rotor thrust will create a right rolling moment, due to the height of the tail rotor, as well as tending to "pull" the aircraft to the right. The mixing unit counters the increase in collective with a negative A_{1s}, or left roll. A third collective mixing is to the longitudinal cyclic pitch, B_{1s}. This

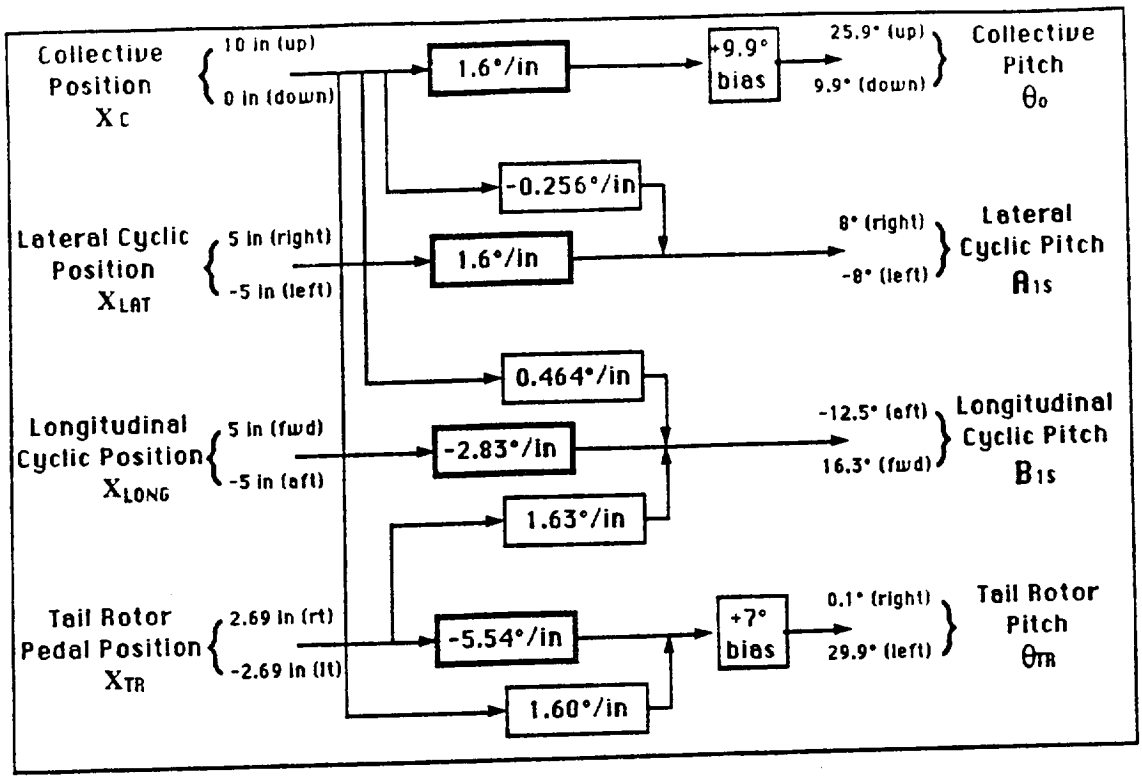

Figure 3-2: UH-60A control system logic, illustrating the control mixing.

mixing provides positive B_{1s}, a nose down pitching moment, to counter the effects of increased downwash on the tail from increased collective, and to counter the tendency for the rotor to flap-back with at forward speed with collective. Also fed to the longitudinal cyclic pitch, B_{1s}, is the input from the directional pedals. This is due to the canted tail rotor. A left pedal input will increase the tail rotor pitch to yaw the aircraft. However, due to the 20 degree cant, the increased pitch on the tail rotor will also provide vertical thrust causing the tail to rise and nose to pitch down. To counter this, the mixing unit provides negative B_{1s}, or nose-up pitching moment.

Outside of the mixing unit, the flight control system on the UH-60A is a redundant hydro-electrical-mechanical system. It includes three dual-stage

main rotor servos to move the swashplate, a dual-stage tail rotor servo, a Stability Augmentation System (SAS), a Flight Path Stability system (FPS), a TRIM feature, and a Pitch Bias Actuator (PBA). The SAS, made up of two independent systems (one analog and one digital), provides short-term dynamic stability through rate damping. The FPS provides a longer term stability to the aircraft through features such as attitude hold, heading hold and airspeed hold. The TRIM maintains the controls at a fixed (trim) position set by the pilot and also moves the controls in response to commands from the FPS. The final part of the flight control system, the Pitch Bias Actuator, is in effect a variable length control rod in the longitudinal cyclic control system that changes the relationship between the cyclic and the tilt of the swashplate. Due to a neutral or slightly negative static longitudinal stability in the unaugmented aircraft, stabilizing at increased airspeeds requires a slight aft movement of the cyclic. The PBA, when operating, compensates for this effect and provides a forward stick movement with increased airspeed while, at the same time, providing the negative (aft stick) input to the swashplate for trim.

The large moveable horizontal tail (stabilator) is automatically programmed to optimize the aircraft pitch attitude for any flight condition and to improve the dynamic response of the aircraft. The incidence angle has a range of from about 40 degrees trailing-edge-down in a hover through about zero degrees at high forward airspeeds to about 10 degrees trailing-edge-up for autorotative descents. The stabilator control system determines the proper angle as a function of four input flight parameters. Variation in collective stick position will require a modified stabilator angle to adjust for the variation in downwash and the change in body angle of attack due to a climb

or descent. Airspeed feedback allows the stabilator to adjust its incidence angle to keep aligned with the airflow. Pitch rate feedback to the stabilator will counter, or dampen, any pitch rates. Finally, sensed lateral acceleration is fed back to the stabilator to reduce pitching moment due to sideslip caused by the non-uniform downwash around the tail.

3.2 USAAEFA Flight Test

The flight test data of the UH-60A, used in validating the model, was obtained in a series of tests conducted by the U.S. Army Aviation Engineering Flight Activity (USAAEFA) at Edwards Air Force Base in 1982 [10]. This flight test program was originally conducted for use in the validation of the Army's Rotorcraft Systems Integration Simulation (RSIS) for investigation of flight control systems, augmentation systems, and displays that are being integrated into modern helicopters. The necessarily high quality of the flight test data, therefore, made it perfect for validation of the analytically linearized helicopter model of this study, without requiring any modifications to the data.

The test program explored steady state and transient responses at various weights, c.g. positions, and velocities ranging from hover to 140 knots. The transient responses are of particular interest for this study, and consisted of individual axis (lateral cyclic, longitudinal cyclic, directional pedal) steps, pulses, and doublets of one inch or less in both directions. The time histories of the control inputs, the test conditions, and the transient responses obtained from the flight test are presented in reference [16]. The aircraft weight was varied in order to set the thrust coefficient (C_T) values as required by the flight test plan. Once in flight, C_T was maintained at the

specified value by increasing the altitude as fuel was expended. Also, the rotor speed was varied as a function of temperature.

The Black Hawk helicopter used in the test program was fitted with the test instrumentation required to vary the trim conditions and to record the necessary data. An airspeed boom was mounted forward of the nose to provide the actual flight airspeed of the aircraft, uncorrupted by the downwash. Elliot Low Airspeed Sensing and Indicating Equipment (LASSIE) was also used in the hover tests for measurement of omnidirectional low airspeeds. A ballast cart was installed and used to maintain lateral and longitudinal c.g. in conjunction with crossfeeding of fuel between the two main fuel cells. Waterline (vertical) c.g. was not controlled in the testing, and was allowed to vary. An instrumented fixture was provided by Sikorsky to measure the three axes of blade motion: pitch, lead-lag, and flap. Reference [10] made note of the fact that after Sikorsky initially calibrated this fixture, the Army had to recalibrate it on a regular basis. This may indicate that the accuracy of that data may be somewhat questionable. There was also a fixture mounted on all axes of the flight controls to allow the vehicle response to a single axis input to be recorded.

The original test plan called for response data on the basic aircraft without the augmentation of the various automatic flight control systems. This unaugmented data was desired to allow validation of a basic simulation model of the aircraft. If augmented data had been collected, the flight control system would automatically alter the transient response making discovery of mathematical modeling errors more difficult. Therefore, during the transient response data runs, no stability augmentation systems were used. Both the analog and digital SAS, the TRIM and the FPS, were disabled, and the PBA

was disconnected and locked in a "mid-length" position. The stabilator was fixed for each run; its position determined as the stabilator control system would have set it for the aim airspeed and collective setting. This allowed proper trim position of the stabilator, but it prevented the automatic features of the stabilator from contaminating the basic response data. Table 2 lists the test plan aim airspeeds and the stabilator position corresponding to each. Ballin [16] noted that the position of the stabilator given in the flight test data

Table 2: Stabilator position setting for the four flight test aim airspeeds.

Aim Flight Airspeed	Stabilator Position (trailing edge down)
Hover	43°
60 knots	31°
100 knots	8°
140 knots	6°

varies up to 5° from these values, and he determined that the aim values as given in table 2 are probably the more accurate ones.

Due to the disabling of all the augmentation systems, the aircraft responses derived in this flight test program should not to be considered representative of a UH-60A Black Hawk in normal operation. They do provide, however, excellent data for validation of unaugmented mathematical models of the helicopter.

The procedure for these flight tests normally consisted of stabilizing in a trim configuration with one of the two redundant stability (SAS) systems on. The allowed for good trim initial conditions. One second prior to control

input the SAS was disengaged, and then the control input was applied. The control fixture, mentioned earlier, allowed for making single axis inputs. The pilot held this configuration until forced to respond due to aircraft acceleration or attitude. Unfortunately, the poor stability characteristics of the unaugmented aircraft, especially in pitch, often prevented the pilot from holding the controls fixed for a long duration. Longitudinal and lateral cyclic inputs as well as pedal inputs often caused divergent pitch response, which caused the pilot to initiate recovery. Because of this, the flight test data is often only useful for five to six seconds.

3.3 Prior Validation of Other Simulation Models

This same flight test data has been used by several different organizations to validate both nonlinear and numerically linearized mathematical models of the Black Hawk. Sikorsky's own GENHEL [9] (for GENeric HELicopter model) is a nonlinear model that also showed reasonable correlation with flight test. It therefore makes a good comparison with the analytically linearized model of this study.

GENHEL was developed by Sikorsky for the Army to do engineering simulations for performance and handling quality evaluations. The model is a total-force, large-angle representation that has six rigid-body degrees of freedom. The modeled rotor system has a hub rotational degree of freedom as well as rotor blade flapping and lagging degrees of freedom for each blade. A blade-element approach is used to model the main rotor blades. No dynamic twisting is modeled, but preformed geometric twist is represented through adjustment of the pitch of each segment of the blade. The total rotor forces and moments are produced by summation of all forces (aerodynamic,

inertial and gravitational) from each blade. These forces are then transmitted through the hub to the fuselage.

The aircraft response to a time varying input is obtained by iteratively summing the components of all forces and moments acting on the aircraft's c.g. and subsequently obtaining the body axis accelerations. These accelerations are integrated through one time step (1/100 second) to produce the resulting velocities and displacements, and then the entire procedure is repeated for the next time step. The results were correlated with the Black Hawk flight test data and found to show reasonable agreement [16]. Numerous deficiencies were noted, however, especially in the off-axis response of the model (e.g. the pitch response to a yaw input).

3.4 Flight Test Correlation of the Original Analytically Linearized Model

The full-order analytically linearized model was compared to flight test to validate its accuracy. A thorough description of the correlation results can be found in reference [13]. Two of the flight test examples are shown in figures 3-3 through 3-8 to demonstrate the capabilities of the model. The graphs indicate the output of the model as originally developed by Zhao and modified by MacDonald. The output of the improved model from this study is provided in Chapter VII.

The first three figures demonstrate the roll, pitch, and yaw rate responses of the helicopter in a hover to a one inch right lateral cyclic input (AEFA Test 201). The full 27 state model including dynamic inflow was used. Correlations are discussed in terms of these fuselage angular rates since their quantities are of primary interest in handling qualities. The roll response, which also appeared in figure 2-8, is shown in figure 3-3. This, being the on-

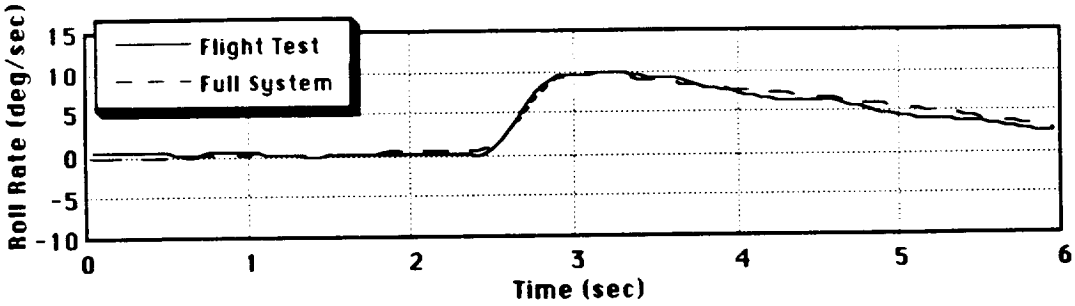

Figure 3-3: Roll rate response of the original 27 state model, with dynamic inflow effects, to a 1" right lateral cyclic input in a hover (AEFA Test 201).

axis response to the lateral input, nearly coincides with the flight test data. This response correlates much better to the flight test than did the GENHEL model in which the response reached a maximum peak of about 40 percent above the flight test value [16]. The off axis responses, figure 3-4 for pitch rate and figure 3-5 for yaw rate, do correlate with the actual helicopter, but not nearly as well as the roll rate. In the pitch axis, the helicopter first pitched down and then up during the flight test. The simulation, however, only pitches up.

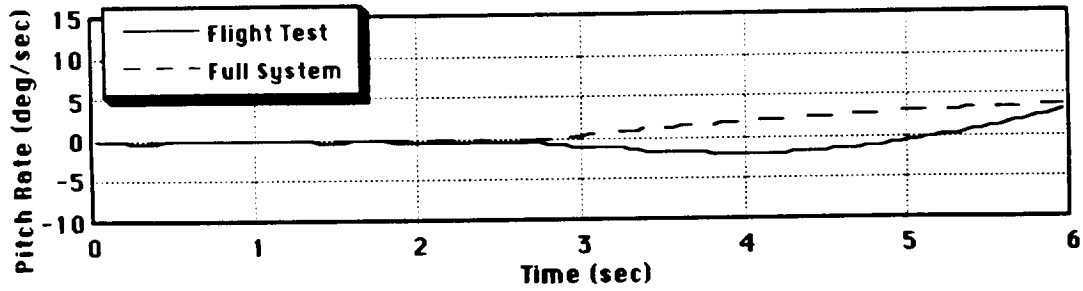

Figure 3-4: Pitch rate response of the original 27 state model, with dynamic inflow effects, to a 1" right lateral cyclic input in a hover (AEFA Test 201).

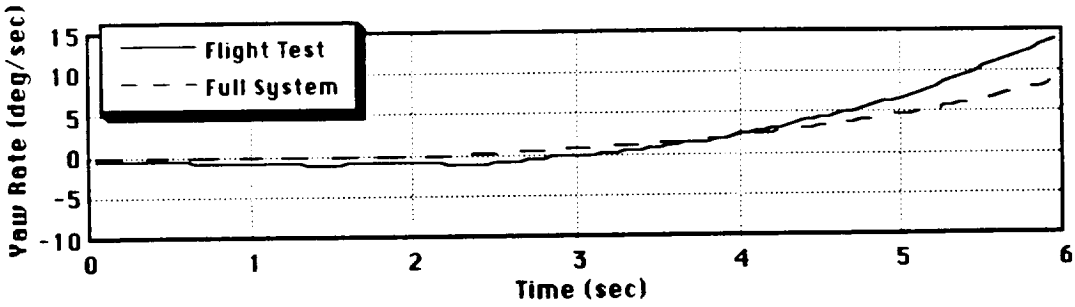

Figure 3-5: Yaw rate response of the original 27 state model, with dynamic inflow effects, to a 1" right lateral cyclic input in a hover (AEFA Test 201).

The model responses to a 1/2 inch doublet pedal input (left pedal first) are shown in figures 3-6, 3-7 and 3-8. The flight velocity is 140 knots (AEFA Test 309). In this case, the roll rate, figure 3-6 is an off-axis response to the

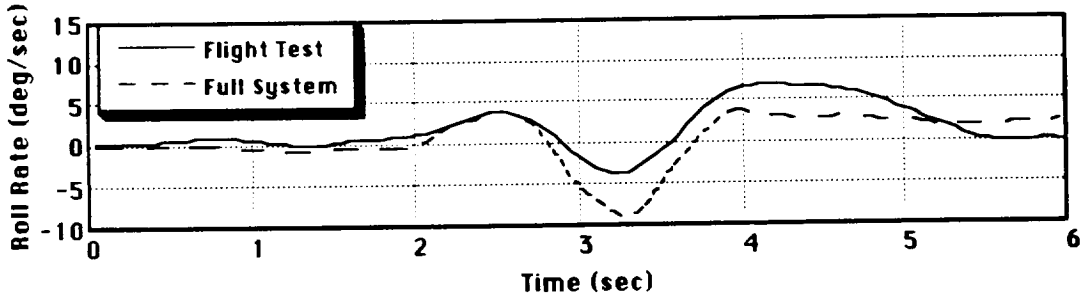

Figure 3-6: Roll rate response of the original 27 state model, with dynamic inflow effects, to a 1/2" left then right doublet pedal input at 140 knots (AEFA Test 309).

pedal input. It correlates with flight test quite well, but there is an overestimation of the roll rate to the left. The pitch rate in figure 3-7 is underestimated and shows much greater nose-down pitching rates after the initial nose-up response. The yaw rate, figure 3-8, is the on-axis response, and shows very good correlation with the flight test. The initial acceleration is not quite as high as flight test, and so the amplitude of the yaw rate at its maximum is smaller.

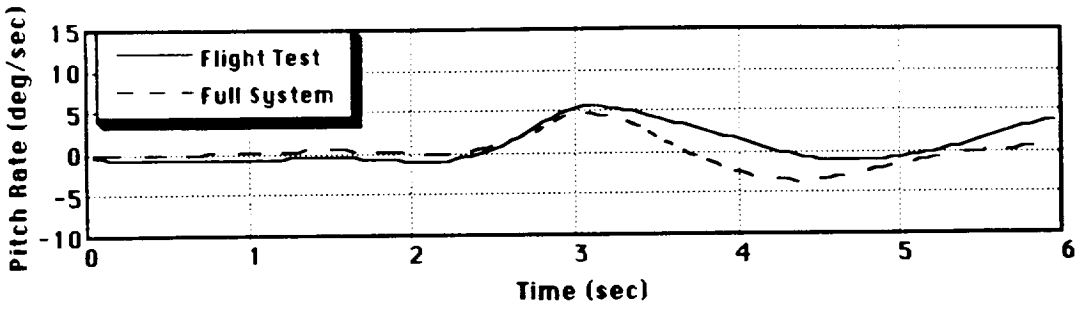

Figure 3-7: Pitch rate response of the original 27 state model, with dynamic inflow effects, to a 1/2" left then right doublet pedal input at 140 knots (AEFA Test 309).

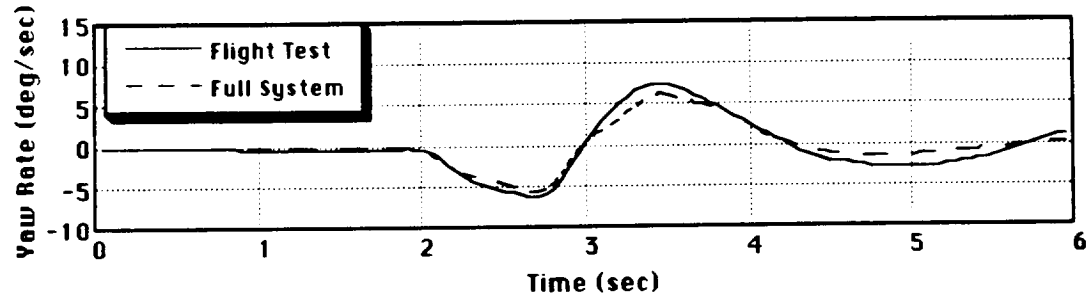

Figure 3-8: Yaw rate response of the original 27 state model, with dynamic inflow effects, to a 1/2" left then right doublet pedal input at 140 knots (AEFA Test 309).

As demonstrated in these graphs, the original model showed good to very good correlation with flight test. In many cases the correlation is better than the output of the much more complicated GENHEL program. Regardless of the comparison to other models, areas still exist that need improvement. Although the on-axis response is very good, deficiencies remain in the off-axis response, and accurate representation of these cross-coupling characteristics of the vehicle are necessary for research relating to flight control. To make the system easier to use, to correct these errors or inconsistencies in the program that reduce its accuracy, and possibly to

improve the correlation with flight test, this research examined three areas: improvement of the computer system interface, corrections in the modeling of the helicopter and in the math model computer code, and improvements in the values input to the program in the trim input file.

CHAPTER IV

MODEL IMPLEMENTATION IMPROVEMENTS

In order for this model to be a useful tool for general use in analysis of helicopter responses, it must be compatible with a large number of computer systems. Ease of use and speed are important aspects as well. It is inconvenient to analyze the sensitivity of the model to variation in a parameter if it is difficult and time consuming to run the model for each value of the parameter. The initial modifications to the model were directed in these important areas.

The implementation of the model as developed by Zhao [1] and modified by MacDonald [11] was neither convenient nor particularly fast, and did not lend itself well to sensitivity analysis. Figure 4-1 shows, in block form, the operation of the original system. The trim input file was developed first from an off-line program and transferred to an IBM 3081 mainframe computer at the Princeton University Computing Center that utilizes the VM operating system. A series of programs written in Fortran IV code on this computer developed the analytically linearized model and created the state-space representation of the system. For time history studies, the system matrices were then transferred to a UNIX based VAX 8700 computer. Programs written in Fortran 77 code on this computer took the matrices and integrated them using a fourth-order Runge-Kutta integration routine with Gill coefficients. The output time histories were then transferred to an IBM or Macintosh PC for plotting. The eigenvalue analysis of the system matrices

required that the files were transferred directly from the IBM mainframe to the PC for analysis. For either the time history or eigenvalue this procedure

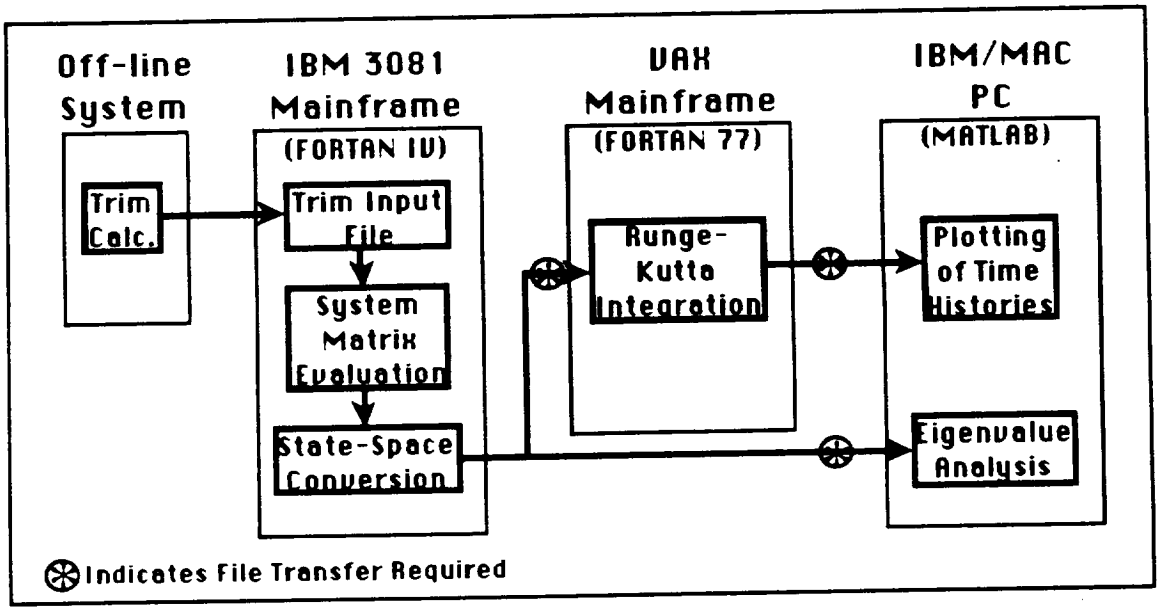

Figure 4-1: Original implementation of the model.

was too complicated and time consuming for easy use. In addition, the variety of computers needed made it impossible to export the system to other research institutions.

Since UNIX based machines are generally available, and have a more "universal" user interface, the mathematical model and associated programs were imported to a UNIX based SUN computer system at Princeton. The programs from the IBM 3081 mainframe were converted from the somewhat antiquated Fortran IV language to Fortran 77, and their user interface was improved. The complicated integration routine was eliminated. A simple but accurate integration routine was combined with the plotting and eigenvalue analysis to be run using a matrix manipulation computer

program called MATLAB, also running on the UNIX machine. Figure 4-2 demonstrates how this simplified the process.

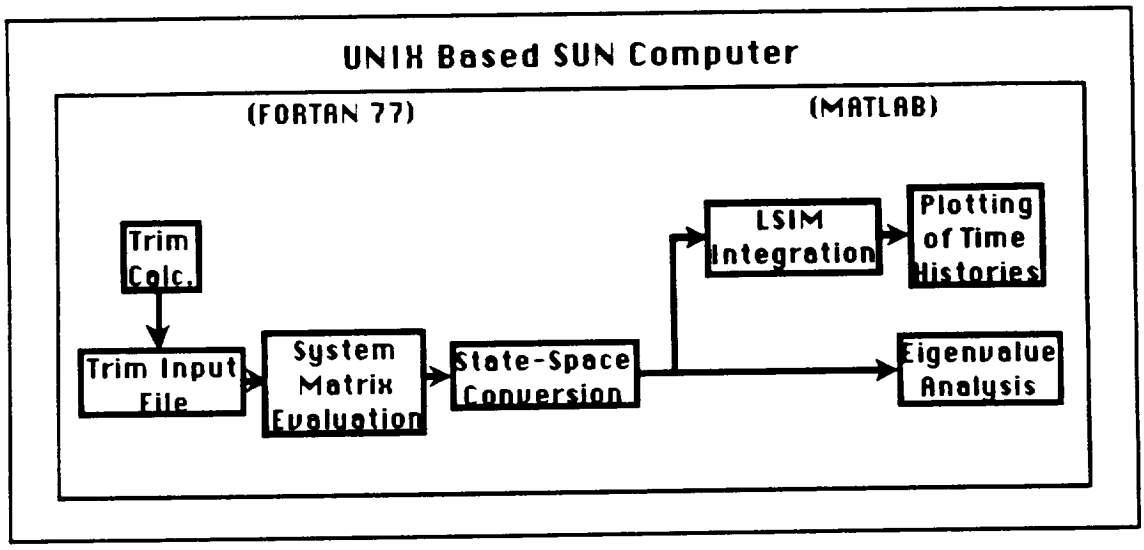

Figure 4-2: Improved implementation of the model.

The trim input file, consisting of data from flight test, wind tunnel data, and a trim program operating on the UNIX system is fed to the main program that develops the mathematical model. The output **A** and **B** matrices are then fed to the MATLAB program, also operating on the UNIX system, for integration and plotting. Instead of using the Runge-Kutta routine from the original system, the state-space representation is integrated using a MATLAB function LSIM. This function is designed to simulate a continuous time linear system with arbitrary inputs. In this case the arbitrary input is the flight test control input history. The LSIM function converts the continuous time system to a discrete time system using matrix exponentials and a specified time step. A step of 0.05 seconds was used as this was the same step size as the control input data and was sufficiently small for good integration results. The function then propagates the response of the discrete

system for the duration of the input. To insure that the discretization process was not degrading the fidelity of the response, plots from the original integration routine and the LSIM routine were compared, and both outputs were nearly identical.

Additional benefits of using the MATLAB program are its plotting capabilities and eigenvalue analysis capabilities. Since it is designed for work with matrices, MATLAB is an exceptional tool for analyzing eigenvalues and eigenvectors. Feedback control systems can be easily implemented and studied, and the output quickly plotted.

These changes to the implementation of the model allow efficient operation of the system and quick and easy sensitivity analysis. Developing and plotting the eigenvalues or response time histories for a series of values of a certain parameter can be completed in a matter of minutes, compared to the hours it took with the original implementation.

Although it may slow the system down somewhat, the entire system should also be exportable to a UNIX based desktop computer that has a Fortran 77 compiler and MATLAB available. However, the size of the System Matrix Evaluation program (see figure 4-2), over 4000 lines of code, may need to be reduced through partitioning in order to meet memory requirements.

CHAPTER V

HELICOPTER MODEL IMPROVEMENTS

Past research with this linearized model has focused on individual aspects that make a significant impact on the time history response correlation with flight test. However, fundamental errors in the model have gone unnoticed. Several of these errors have been discovered and corrected to improve the accuracy of the model.

5.1 Rotor Forces Resolved to the Body

As discussed in the description of the rotor and fuselage degrees of freedom, care must be taken when transmitting forces and moments from the rotor hub axis system which is unconventional, although right-handed, to the fuselage axis system which is left-handed. These fuselage axes, previously defined in figure 2-3, are aligned with the waterline/frame-station/butt-line reference system.

This reference system, adopted from ship design, uses these terms to depict positions in the Z, X, and Y axes respectively. See figure 5-1. The waterline position, analogous to the waterline of a ship, defines a horizontal plane where the ground or a plane below the ground is given a value of zero. Every position on the aircraft has a positive waterline value that indicates the number of inches above the zero level. The frame-station is similarly defined for the position along the longitudinal axis. In this case, the zero position is out in front of the nose, so all positions are a positive number of inches

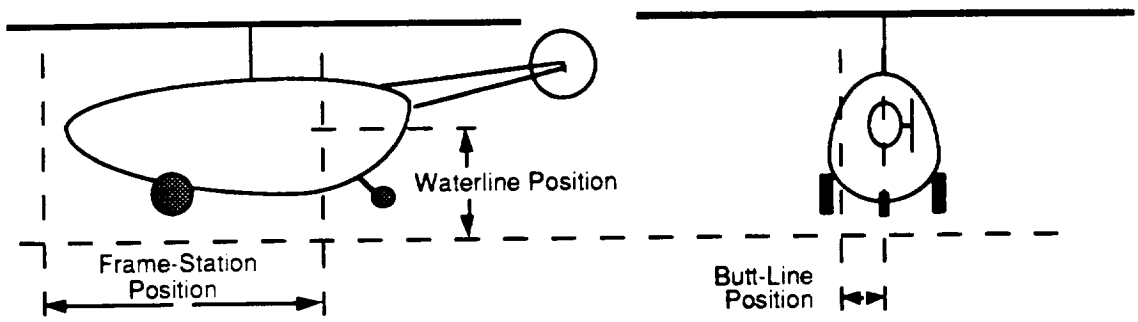

Figure 5-1: Definition of the waterline/frame-station/ butt-line reference system.

behind that point. Finally, the butt-line system defines left to right position where the centerline of the aircraft is zero. There are both positive and negative values for the butt-line to indicate number of inches right and left of the centerline respectively. All linear dimensions for the helicopter are given in this reference system.

The conversion between the fuselage center of mass (c.m.) motion and the hub motion in the model is performed through a transformation (T) matrix. Figure 5-2 shows the geometry that the T matrix uses for the

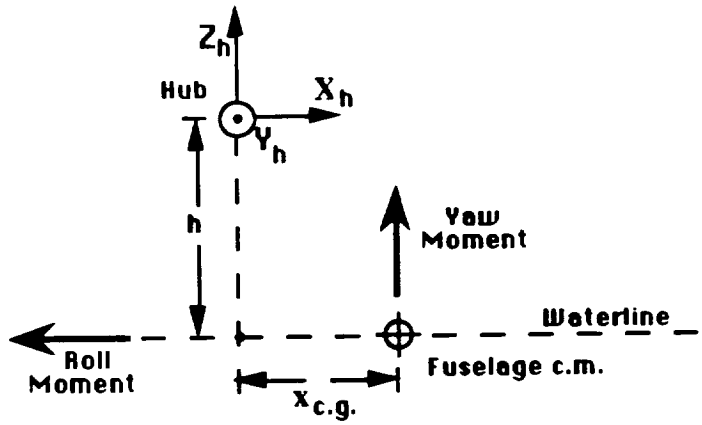

Figure 5-2: Hub and fuselage c.m. geometry.

conversion, according to,

$$X_{hub} = T\, q_b, \tag{5.1-1}$$

where

$$\mathbf{X}_{hub} = [\theta, \phi, \psi, y, x, z]_{hub}^{T} \text{ and } \mathbf{q}_b = [\theta, \phi, \psi, y, x, z]_{body}^{T}, \qquad (5.1\text{-}2)$$

the latter being defined as in section 2.5. The **T** matrix has the values,

$$\mathbf{T} = \begin{bmatrix} 1 & 0 & 0 & 0 & 0 & 0 \\ 0 & -1 & 0 & 0 & 0 & 0 \\ 0 & 0 & 1 & 0 & 0 & 0 \\ 0 & h & -x_{cg} & 1 & 0 & 0 \\ h & 0 & 0 & 0 & 1 & 0 \\ x_{cg} & 0 & 0 & 0 & 0 & 1 \end{bmatrix} \qquad (5.1\text{-}3)$$

where x_{cg} and h are defined in figure 5-2 with a positive x_{cg} for a fuselage c.m. aft of the hub. The aforementioned change of sign between the hub roll angle and the fuselage roll angle is accounted for by the value of -1 in T(2,2). The other terms follow the geometry exactly.

Since the rotor forces and moments are initially resolved into the shaft axis, this transformation would be suitable for a shaft that coincides with the Z_{body} direction. This model, however, is designed to take a shaft tilt (called AN in the program) into account. As depicted in figure 5-3, this tilt changes the geometry of the problem somewhat. The most obvious change that the tilt makes, is to move the line of force of the thrust vector, thereby changing the moment arm for its affect on the pitch moment. To account for this, the original derivation of the model included terms to change the fuselage pitching moment due to the rotor forces,

$$\text{Pitch Moment} = (H_s \cos(AN) - T_s \sin(AN))\, h + T_s \cos(AN)\, x_{cg} \qquad (5.1\text{-}4)$$

simplified via small angle approximations to,

$$\text{Pitch Moment} = (H_s - T_s\, AN)\, h + T_s\, x_{cg}. \qquad (5.1\text{-}5)$$

The other moments were unchanged in the original model,

$$\text{Roll Moment} = Y_s\, h \tag{5.1-6}$$

$$\text{Yaw Moment} = -Y_s\, x_{cg}. \tag{5.1-7}$$

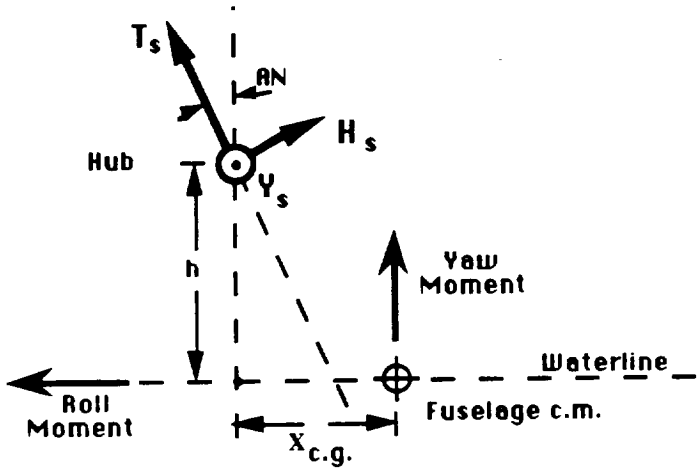

Figure 5-3: Geometry for a shaft tilted by the angle AN.

This change properly corrects the calculation of the fuselage moments generated by the rotor system. However, since the T matrix is also used in resolving rotor motions, forces and moments into the fuselage frame, the shaft tilt was still causing errors in this resolution. A slight coupling occurs between the components of motion (translational and rotational) in transforming between the tilted shaft hub and the fuselage. Since coupling is a problem noted in the original flight test validation [13], any corrections in this area should be of benefit.

During this research, the original terms that had been inserted in the pitch moment equation were removed and a complete axis transformation was made. This corrected all three axes of the system by taking the value of AN into account. The new T_{new} matrix converts between the fuselage c.m.

and the tilted shaft systems,

$$\mathbf{X}_{shaft} = \mathbf{T}_{new}\, \mathbf{q}_b, \tag{5.1-8}$$

and has the values,

$$\mathbf{T} = \begin{bmatrix} 1 & 0 & 0 & 0 & 0 & 0 \\ 0 & -\cos(AN) & \sin(AN) & 0 & 0 & 0 \\ 0 & \sin(AN) & \cos(AN) & 0 & 0 & 0 \\ 0 & h & -x_{cg} & 1 & 0 & 0 \\ h & 0 & 0 & 0 & \cos(AN) & \sin(AN) \\ x_{cg} & 0 & 0 & 0 & -\sin(AN) & \cos(AN) \end{bmatrix} \tag{5.1-9}$$

where the $T_{new}(2,2)$ still includes the -1 for reversal of the roll angle. For a helicopter with no shaft tilt, this reverts back to the original definition of **T** (equation 5.1-3).

This change to the T matrix corrects for the oversight in the incorporation of AN in the original derivation of the system, thereby increasing the accuracy of the system. When the system response to the flight test input was plotted, it indicated an improvement in the correlation with flight test, but the improvement was slight. The model was improved to ensure that the physics were correct, but due to the small angles involved, it did not make a large impact on the overall system response.

5.2 Trim Force and Moment Correction

Although it is true that the linearized model should not be sensitive to small variations in the trim flight condition, the better the accuracy of the trim calculations and input, the more accurate the response. In the case of the nonlinear models, such as GENHEL, only flight initial conditions (velocity, weight, etc.) are specified and the program calculates the resultant rotor forces

and moments required to attain that flight condition. From this, the value of rotor and body angles are calculated. The analytically linearized model with its trim input file, on the other hand, tends to work in reverse. It takes the rotor and body angles that are input to the system, calculates the resultant forces and moments from them, and then uses these values in the derivative formulation. It is important, therefore, that the calculations are correct and derive accurate values of the forces and moments. The interpretation of these trim rotor forces and moments are shown in figure 5-4.

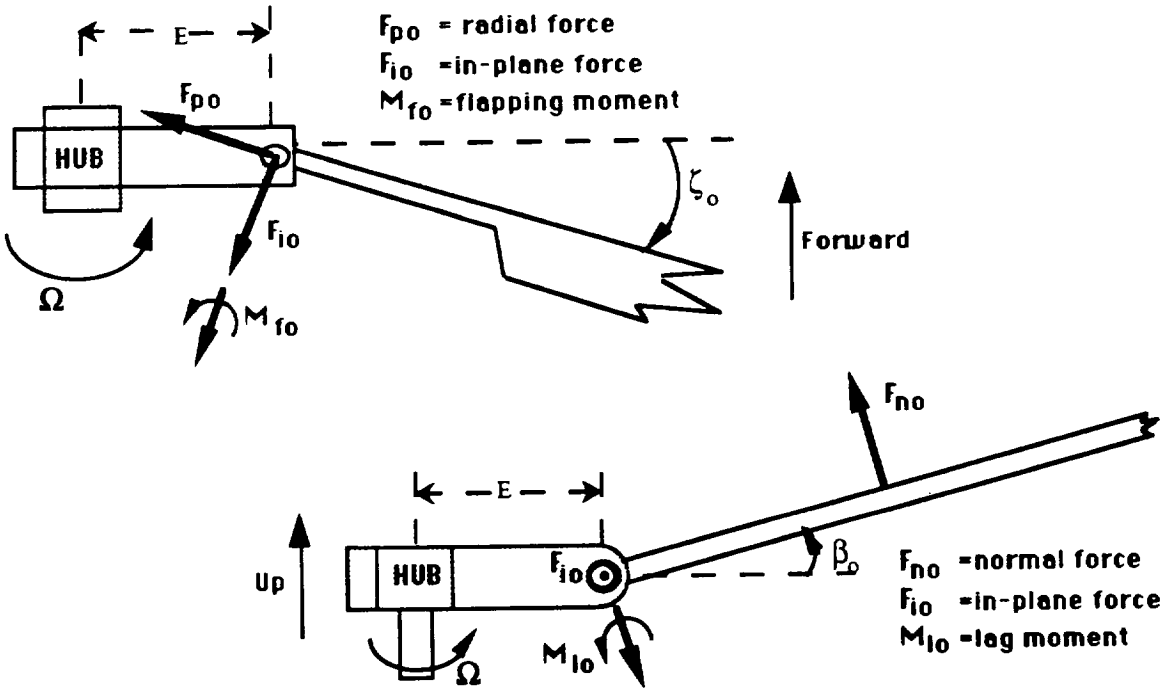

Figure 5-4: Calculated forces and moments on the blade and hub.

To verify the accuracy of the trim force and moment calculations, the value of the rotor thrust and power required by the rotor, as determined by the model, were output. These values come directly from the forces and

moments depicted in figure 5-4 as,

$$\text{Thrust} = F_{no} \cos(\beta_o) * (4 \text{ blades}) * a, \tag{5.2-1}$$

$$\text{Power}_{req} = (E *(F_{io} \cos(\zeta_o) - F_{po} \sin(\zeta_o)) + M_{lo} \cos(\beta_o))* (4 \text{ blades}) * \Omega * a, \tag{5.2-2}$$

where a is a constant (the value of rotor blade lift slope) needed to properly dimensionalize the forces as used in the program. The outcome of these calculations are listed in table 3 for three different flight velocities and weights.

Table 3: Outcome of initial trim calculations.

Flight Velocity	Aircraft Weight	Calculated Thrust	Calculated Rotor Power_{req}
Hover	15750 lbs	16550 lbs	1851 hp
60 knots	16110 lbs	13940 lbs	1048 hp
140 knots	16300 lbs	28260 lbs	1829 hp

The values of calculated power required by the main rotor appear reasonable considering that the UH-60A engines are each capable of producing nearly 1600 hp [10]. Total power required from the engines would be 10 to 15 percent above the value for the rotor in table 3. The Black Hawk should not generally be capable of single-engine hover nor single-engine flight near V_{max} at these weights, but the helicopter should be capable of flight in mid-range airspeeds with one engine inoperative. The calculated power correctly indicates this. The other calculated value, thrust, should be approximately equal to the aircraft weight. However, this does not hold true at the higher airspeed. At 140 knots, the trim thrust calculated by the program is nearly double the weight of the aircraft; an obvious error.

The equations used by the program for calculating F_{no} were examined to determine if an error was present. Although they had inconsistencies in comparison with simplified theory as given by Gessow and Myers [12] they did agree (in somewhat simplified form, i.e. neglecting the hinge offset) with the more detailed Bailey theory as detailed in reference [17]. A sensitivity analysis was therefore performed to determine if an incorrect input parameter value was causing the discrepancy.

It was soon found that substantially increasing the value (in a negative or nose-down sense) of the body angle of attack, (α_B), from that given in the flight test served to bring the calculated thrust more in line with the weight. However, a change in strictly the body angle of attack should not have a significant effect on this calculation. Since the angle of attack of the rotor shaft, α_S, is related to the fuselage angle by the shaft tilt angle, AN, according to

$$\alpha_S = \alpha_B - AN, \tag{5.2-3}$$

modification of the body angle was pitching the rotor system down as well as the body. It was this change in angle of attack of the rotor that improved the calculations. The original values of α_B and AN being used were determined to be correct, so it was realized that the error was in specifying the rotor attitude in terms of α_S. The control axis angle of attack, α_{CA}, which takes the value of B_{1S} into account,

$$\alpha_{CA} = \alpha_S - B_{1S}, \tag{5.2-4}$$

more appropriately specified the rotor attitude. Figure 5-5 graphically illustrates how these variables are related.

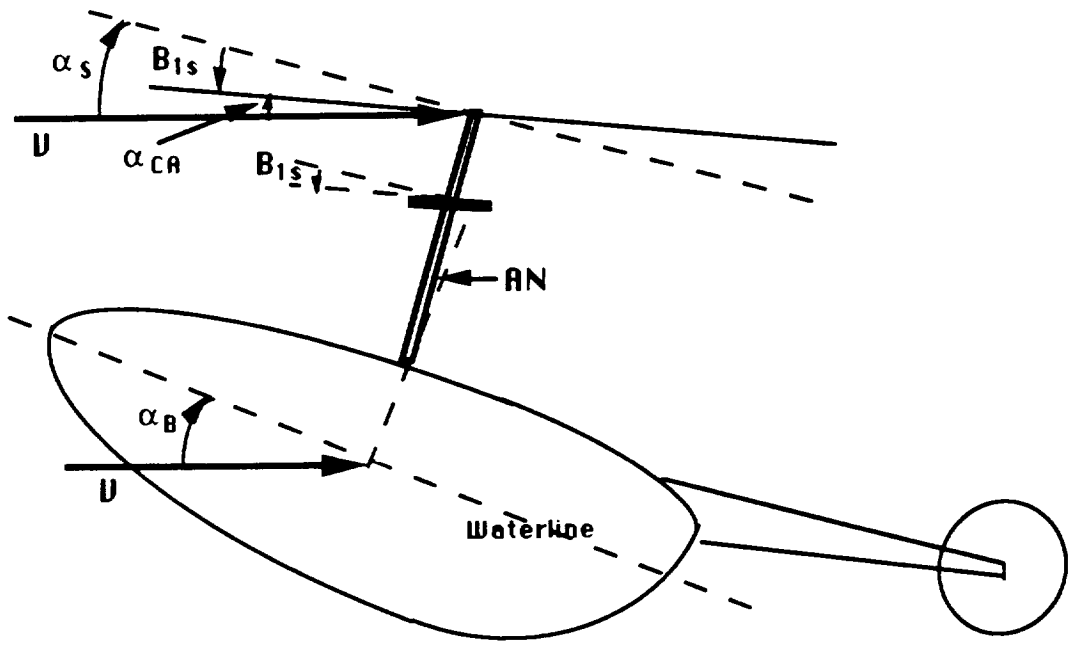

Figure 5-5 Body, shaft, and control axis angles of attack.

In the original formulation of the model, it had been assumed that the value of B_{1s} in trim would be small, and therefore it was neglected in the calculations. In Ballin's study on modeling the Black Hawk [16] he indicated that the longitudinal position of the cyclic remained relatively constant at a range of airspeeds. This was due to the aforementioned neutral speed stability of the aircraft for which the PBA (as discussed in section 3.1) was designed. Neglecting the trim B_{1s} seemed, therefore, to be an appropriate assumption.

What wasn't considered, however, was the input to B_{1s} made by the trim collective and pedal positions via the mixing unit illustrated in figure 3-2. Determined from the work of Curtiss [18] and Cooper [15], the equation for B_{1s} is approximately,

$$B_{1S} = 0.464\, X_C - 2.83\, X_{LONG} + 1.63\, X_{TR}. \qquad (5.2\text{-}5)$$

Utilizing the values from flight test for the collective (X_C), longitudinal cyclic (X_{LONG}), and pedal (X_{TR}) positions at 140 knots, a B_{1S} of about 6.7 degrees results. Then, to further check this value of B_{1S}, the value of individual blade pitch, θ, was plotted from flight test as shown in figure 5-6. This graph shows, although somewhat crudely due to the low sampling rate, that in the trimmed flight before an input was made, the pitch oscillated around a steady

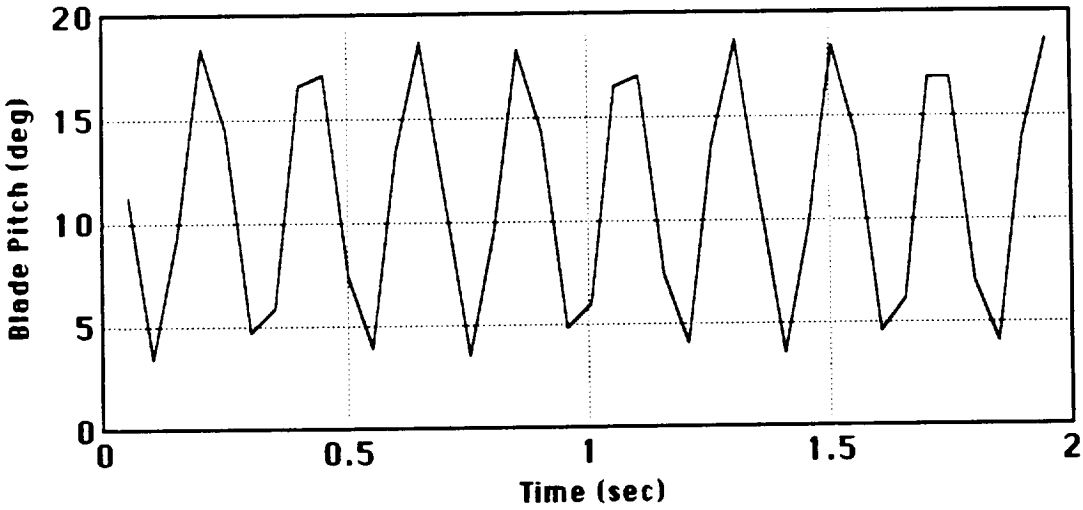

Figure 5-6: Blade pitch angle for trim flight at 140 knots (AEFA Test 309).

state value. Since there was very little lateral stick displacement during these tests, and A_{1S} is almost entirely defined by the lateral stick position,

$$A_{1S} = 1.6\, X_{LAT} - 0.256\, X_C, \qquad (5.2\text{-}6)$$

the equation for blade pitch (2.2-4) would indicate that the oscillations are due to B_{1S}. The value of B_{1S} can therefore be approximated from the graph at

about 7.7 degrees. Because the blade angle measurement device had to be recalibrated repeatedly during the flight testing, and the system measured the pitch at the cuff and not at the root of the blade, the steady state value on the graph is not the same as θ_0. The value of B_{1s}, however, should be correct. The discrepancy between the 6.7 and 7.7 degrees most likely comes from the fact that the PBA was locked at an unknown "mid-length" position. Since the PBA, in effect, changes the length of the control rod from longitudinal cyclic to the swashplate, its configuration can create the biasing effect that is noted. The calculated and flight test values of B_{1s} for several tests were examined to determine an average bias which was used to correct equation 5.2-5,

$$B_{1s} = 0.464\, X_C - 2.83\, X_{LONG} + 1.63\, X_{TR} + 1.27°. \qquad (5.2\text{-}7)$$

The importance of B_{1s} in the calculations was accounted for in the model by modifying the angle of attack used in the trim force and moment equations. The value of trim B_{1s} was added to the trim input file, the control axis angle of attack α_{CA} was calculated from the trim B_{1s}, and then the angle of attack terms in the trim force and moment equations were changed to α_{CA}.

The outcome of these changes was a trim thrust calculation that much better approximated the value of aircraft weight at high airspeed. The thrust at the lower airspeeds are not quite as close to the weight as before, and the power required calculation changed slightly, but they all remained in an acceptable range. Table 4 indicates these corrected values.

By the assumption that we can linearize the system around a trim value of the flight condition, a change of eight degrees to the angle of attack of the rotor should only have a small impact on the aircraft response to an input. Plotting the response of the model to flight test inputs for the model

with and without a trim B_{1s} value did, in fact, confirm that the change to the response was minor. However, the overall accuracy of the model has definitely been improved.

Table 4: Outcome of corrected trim calculations.

Flight Velocity	Aircraft Weight	Calculated Thrust	Calculated Rotor $Power_{req}$
Hover	15750 lbs	17600 lbs	1812 hp
60 knots	16110 lbs	13390 lbs	1072 hp
140 knots	16300 lbs	17120 lbs	1673 hp

5.3 Rotor Inertial Velocity Terms

A third change made to the model during this research is in the calculation of rotor system inertial variables. Due to the fact that the model is based in a space-fixed frame, the velocity of the helicopter, V, should not impact the rotor inertial variables as would happen in an Eulerian frame. Analysis of the inertial variables indicated that, indeed, terms dependent on V had crept into the equations. These terms were removed from the equations to correct the error.

5.4 Style Improvements

In many other areas of the code, programming style was corrected and updated in order to increase the understandability of the program as well as increase the efficiency and speed.

In general, the only variables specifically declared in the program were those that required dimensionalization as a matrix or vector. All others were

left to the Fortran default type. In three cases variable names beginning with either an M or an L were for variables that were to be defined as real. Fortran automatically defines variables with those initial letters as integers. This discrepancy went unnoticed although it caused the values of these variables to be incorrectly set at zero. Properly defining the names corrected the problem and the variables were able to be used normally.

In several other cases, the same names were inadvertently used for different variables in different parts of the program. The calculations involving these variables were sufficiently independent to prevent an incorrect result, however, it became difficult for the user to understand the program. These variables names were changed.

Finally, in order to make the programs more efficient, numerous constant terms like $\cos(\beta_o)$, $\sin^2(\beta_o)$, and Ω^2 that were calculated and recalculated hundreds or thousands of times throughout the program were modified. Instead, they are calculated once at the beginning of the program, assigned to a new variable name such as cbeta0, sbeta0sqd, or omegasqd, and then these variable names were used for the duration of the program.

Each of these changes served to improve the performance or accuracy of the program, while at the same time improving the understandability for the user.

CHAPTER VI

TRIM INPUT FILE FOR THE SYSTEM

The analytical linearization process used in this research produces a model that is independent of a specific type of helicopter or a specific trim condition. After the model has been generically developed, the process of inputting a trim input file allows the model to produce a state-space representation that is the response of a certain type of helicopter around a certain trim condition.

The accuracy of the different types of information in this trim file has different effects on the model output. Small variation in the input trim conditions of the helicopter may only create a small variation in the output. However, errors in other parts of the input file could make an impact. Incorrect physical configuration or physical size values, for instance, can change the output more significantly.

6.1 Stabilator Incidence Angle

A sensitivity analysis on the stabilator incidence angle provides an example where the accuracy of the trim value has very little effect on the outcome. In studying a version of the nonlinear GENHEL model, Ballin [16] determined that the value of stabilator incidence angle had a significant effect on the nonlinear model response, especially in the trimmed flight calculation. He reported that errors in this value had caused miscalculations in the flapping and lagging response of the rotor in earlier studies. The

analytically linearized model was therefore studied to see if it too had this strong dependence. It was determined that it did not.

Admittedly, the absolute value of the trim lift on the stabilator will be different for two cases in which the incidence angle is different. However, the other trim values of the aircraft are dependent on the input in the trim file and not on the value of stabilator lift. In both cases, the model would give continued steady state flight in the absence of an outside input. When the inputs are applied, they are perturbational inputs, so, for example, a longitudinal cyclic input would cause a perturbational change of aircraft pitch from the steady state condition. This pitch change would affect the above two cases by changing their angle of attack by the same perturbational amount, $\Delta\alpha$. Since lift is basically a linear function of angle of attack,

$$\Delta C_L = C_{L\alpha}\,\Delta\alpha \tag{6.1-1}$$

both cases would have the same perturbational lift generating the same perturbational pitching moment, and there would be no difference between the responses. Of course, if the basic relation was nonlinear, some difference between the two cases would occur, but since the perturbations are considered very small the difference would be very small.

This simplified view of the stabilator helps to explain some of the value in using a linearized model. Use of the stabilator angle values that Ballin considered inaccurate had little effect on the model. However, just to maintain overall accuracy of the model, the values were changed to the more accurate ones.

6.2 Linear Geometric Twist

An item in the trim file that can make a large difference in the aircraft response is the geometric twist built into the main rotor blades. The value of linear twist in the input file is given in units of degrees of twist per foot along the blade. An incorrect value of twist in the model will cause errors in all main rotor thrust, moment and torque calculations, thereby severely impacting the accuracy of the results.

For the Black Hawk, the value of blade twist is given as a linear "-18° (equiv)" [10] which would imply that

$$\text{twist/ft} = -18°/26.83 \text{ feet} = -0.671 °/\text{ft} \tag{6.2-1}$$

where 26.83 feet is the rotor radius. The original trim input files, therefore, used this value for the twist. In the model, the rotor blade is considered as a rectangular blade with a constant linear pitch from the hinge to tip, so for a root pitch of zero degrees this resulted in a tip washout of over 17 degrees. (There is no twist up to the first 1.25 feet of radius where the hinge is located.) Reference [9] indicates that the blade does have a -0.671 °/ft twist, but only starts the twist at the beginning of the blade surface which is 5.4 feet from the hub center. This results in a tip that is washed out only about 14.5 degrees. Figure 6-1 shows the shape of the UH-60A main rotor blade, the shape of the modeled blade, and has the blade twist graphed. The difference between the actual tip washout and the value used in the trim input file has a substantial effect on the thrust developed by the blade. For the same root pitch, this incorrectly modeled blade will produce much less lift, overall, than the actual blade.

Since blades on different helicopters are designed differently, a

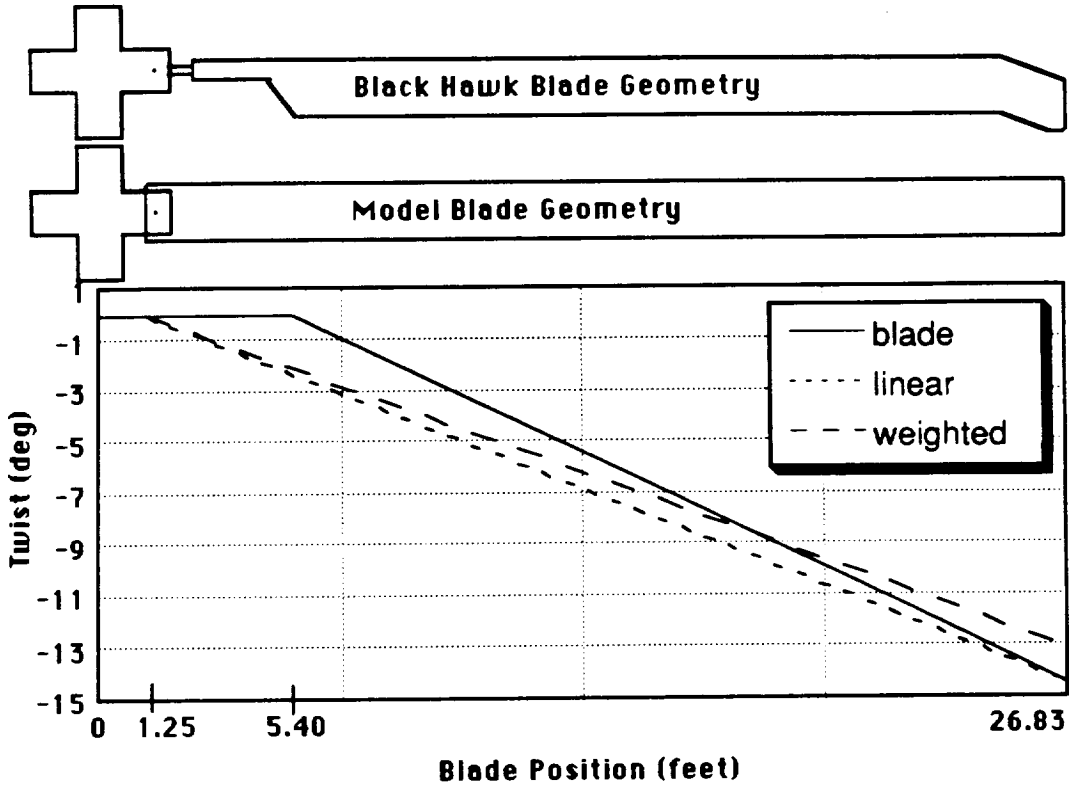

Figure 6-1: Geometric blade twist for the actual and modeled blade.

conversion of the actual blade geometry and twist to a full rectangular blade with linear twist must be made before a value is used in the input file. As shown in figure 6-1, a strict linear twist from hinge to tip for the same tip washout results in a blade that has a greater washout throughout the length than the actual blade. This also will cause an undercalculation of the thrust. To properly calculate the equivalent twist for the model, a nominal lift must be integrated across the helicopter blade, according to the design of the blade, to determine a value of total thrust. A value of twist for the modeled blade must then be derived to achieve this same value of total thrust. The plot of "weighted" twist in figure 6-1 shows the appropriate calculated value of - 0.51°/ft.

This change in twist, which causes an overall change in thrust, does have a significant impact in all the model calculations. The figures in Chapter VII of this report indicate how the response was substantially affected due to the corrected value of the linear twist. The calculations of section 5.2 concerning B_{1s} were performed using this corrected value of twist.

6.3 Control System Input Phase Angle

The helicopter control system is designed to transfer the pilot's input to the swashplate which in turn changes the pitch on the blades. Obviously, a pure lateral input should create a pure rolling motion in the blades. However, due to the steady state lag on the blades, this may not always be true. A control system input phase angle, Δsp, is therefore used on the Black Hawk to compensate. Figure 6-2 illustrates the effect of the lag. Part (a) of the figure shows the rotor system without the phase angle compensation. Pure lateral input to the rotor causes maximum roll deflection of the blades when the hub is at $\Psi=90°$. However, due to the steady state lag, ζ_o, the blade achieves this maximum deflection at $\Psi=90° - \zeta_o$, causing a small longitudinal pitch-up response as well.

This can be the cause of some of the cross-coupling noted in the original validation of the model with flight test. Although the roll input can cause a longitudinal response, a pitch input also can cause an even greater lateral response due to the aircraft's lower moment of inertia in roll.

In part (b) of figure 6-2, the effect of the input phase angle is shown. The lateral input is rotated a number of degrees forward ($\Delta sp=9.7°$ [9]) to $\Psi=90° + \Delta sp$. If the lag has the same value, then the lateral input will create the maximum roll deflection in the blades at $\Psi=90°$ giving purely roll

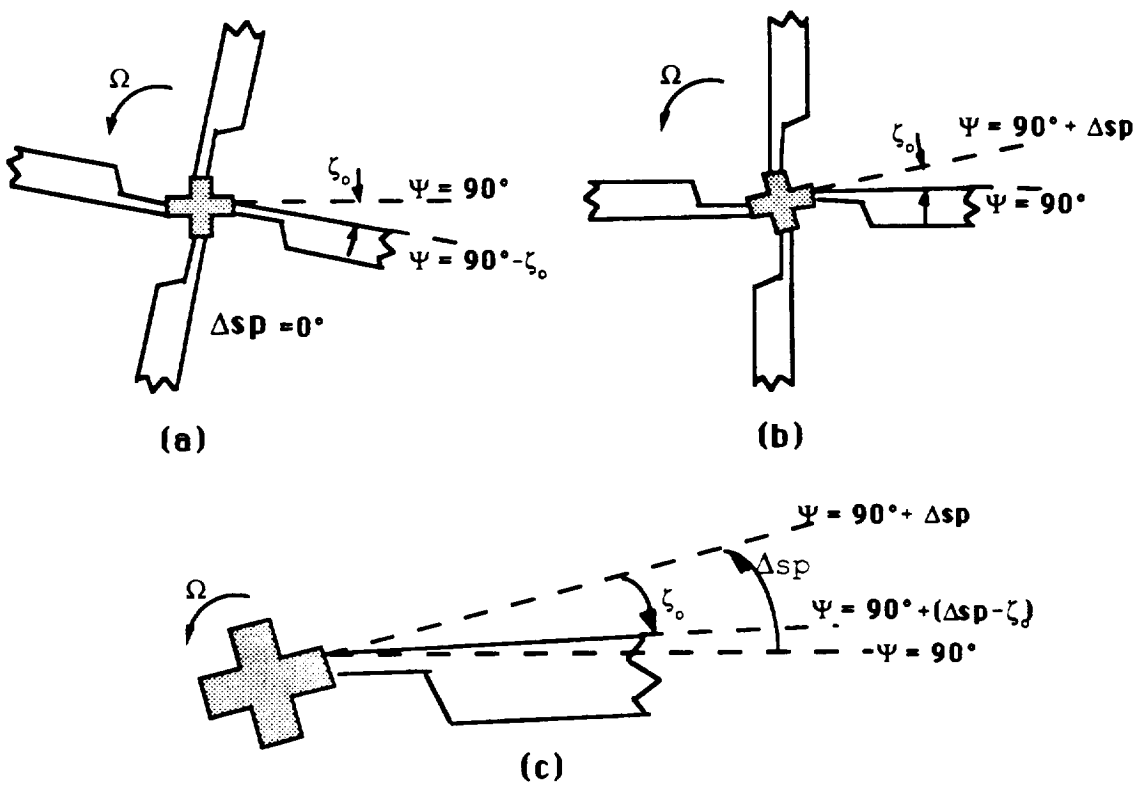

Figure 6-2: Control system input phase angle, Δsp.

motion. The same correction would work for a pitch input. Unfortunately, the steady state lag is variable with flight condition, and in many cases for the Black Hawk is about 5 to 7 degrees. This creates a situation as in figure 6-2 (c) where the input phase angle has over compensated for the lag, thereby again causing some cross-coupling in the axes. However, the degree is much reduced. Time histories in Chapter VII illustrate the improvements due to correct use of Δsp.

6.4 Steady-State Coning and Lag Angles

In the flight test, the trim steady-state values of main rotor coning and lag were measured by a device mounted on the blades. Having been noted as a device needing frequent recalibration, the absolute values of these angles

were in question. To ensure accuracy in the model, therefore, these angles were instead calculated from the moments of the blade acting in their direction.

Figure 6-3 illustrates the origin of the moments acting on the blade: Thrust, Drag, Weight, Inertia, Centrifugal Force, and Hub Springs. For the Black Hawk, since there are no hub springs, M_{hs} is zero. For steady state

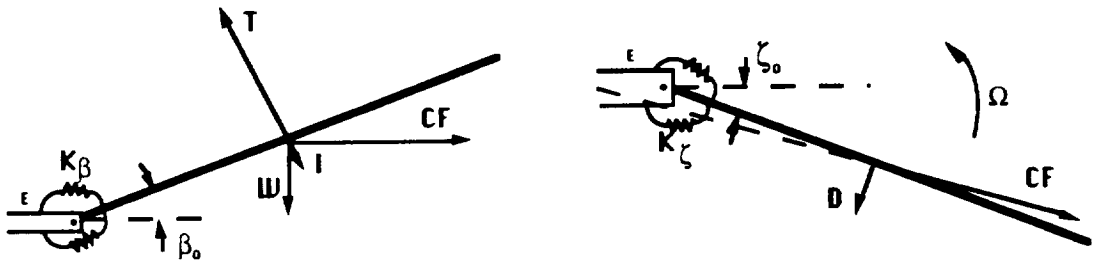

Figure 6-3: Forces generating coning and lag.

conditions, the sum of the moments must be zero, or

$$M_t - M_w - M_{hs} = M_{cf} + M_i. \tag{6.4-1}$$

The physics of the problem can be calculated as,

$$M_{cf} + M_i = m_b \Omega^2 R^3 \beta_o / 3. \tag{6.4-2}$$

Substitution of the blade inertia, $I_b = m_b R^3/3$, and equation 6.4-2 into 6.4-1 yields,

$$\beta_o = (M_t - M_w - M_{hs})/I_b \Omega^2, \tag{6.4-3}$$

which calculates the steady state coning angle. However, these calculations did not take the hinge offset, e, into account. This offset will change equation

6.4-3 to,

$$\beta_o = (M_t - M_w - M_{hs})/(E\, S_b - I_b)\, \Omega^2 \qquad (6.4\text{-}4)$$

where S_b is the blade first mass moment. In a similar manner, the equation for steady state lag can be calculated as,

$$\zeta_o = (M_d - M_{hs})/\, S_b\, E\, \Omega^2. \qquad (6.4\text{-}5)$$

The model calculates the trim values of M_t (MFO*a) and M_d (MLO*a) in the development of the various derivatives that depend on their values. These values can therefore be used to calculate the steady-state coning and lag angles for input in the trim file. However, to ensure the accuracy of MFO and MLO, their values were compared to manual calculations of the thrust moment and lagging moment using the linearized Bailey theory. The difference between the values at various flight conditions was determined to be very small, and therefore the values of MFO and MLO were used.

The corrected values of β_o and ζ_o were up to a degree different from those originally used. As determined by MacDonald [11], the change in lag angle has an effect on axis cross-coupling only due to the effect in conjunction with Δsp. Without this effect on the input phasing, variation in ζ_o has little effect on the response. The change in coning also has little impact on the response due to the linearization around the trim value of coning.

6.5 Main Rotor and Tail Rotor Pitch

The values of main and tail rotor pitch were originally derived from the flight test values of the control settings. The mixing unit shown in figure 3-2 converts these flight control settings to the the main rotor collective pitch θ_o and the tail rotor pitch θ_{TR}., according to

$$\theta_0 = 1.6\, X_C \tag{6.5-1}$$

$$\theta_{TR} = 1.60\, X_C - 5.54\, X_{TR} + 7°. \tag{6.5-2}$$

To ensure that the values derived in this manner were not in error, manual calculations were performed. To check the main rotor collective pitch, linearized Bailey equations were used to solve for θ_0 as a function the thrust required to counter the weight of the aircraft. Nearly identical values of collective pitch were derived in the two manners, allowing the conclusion that equation 6.5-1 is a reasonable approximation for collective pitch.

For the tail rotor pitch, the value derived from the directional pedal position was compared to a value manually calculated from the tail rotor thrust required to counter the torque of the main rotor. Linearized Bailey theory was again used, and to account for the tail rotor δ_3 hinge, equations developed by Seckel and Curtiss [19] were used. These manual calculations again produced values that were very close to those calculated in equation 6.5-2. It was therefore concluded that equation 6.5-2 is a good approximation for the tail rotor thrust.

6.6 Uniform Induced Velocity

Once the main rotor thrust and tail rotor thrust had been determined, the values of uniform induced velocity could be directly calculated for both the tail rotor and main rotor as,

$$v_0 = C_t\, \Omega\, R \,/\, 2(\lambda^2+\mu^2)^{1/2}, \tag{6.6-1}$$

which can be approximated by

$$v_0 = \Omega\, R\, (C_t/2)^{1/2} \tag{6.6-2}$$

in the hover case and

$$v_o = C_t \Omega R / 2\mu \tag{6.6-3}$$

for airspeeds greater than about 50 knots. λ is calculated as

$$\lambda = (V \sin \alpha - v_o)/\Omega R. \tag{6.6-4}$$

The source of the original values for main and tail rotor v_o, which is somewhat different from these calculated values, is unknown, however, the values as derived from the above equations were used in the trim input file. Changing from the previous values to these values had only a small effect on the response.

6.7 Other Corrections

In addition to the sensitivity analyses and manual calculations performed to check for changes to the inputs, all other values in the trim input file were also checked for accuracy. Slight errors in physical dimensions and flight test conditions, such as velocity and c.g. position, were discovered and corrected. Of these, only the change in velocity that occurred on three of the cases had an impact on the response as compared to the original validation.

CHAPTER VII

RESULTS OF THE CHANGES

During this research, numerous changes were made to this analytically linearized model and to the trim input file that drives it; each with the goal of improving the accuracy of the model. Since this model has undergone extensive research in the past, many of the major problems that would affect model response have been already corrected. The changes made in this research are generally of a more subtle kind, that improve the physics of the problem and improve the overall accuracy of the results, but may not have a significant visual effect on the model response for the Black Hawk. Several of them, most notably twist, have improved the response dramatically. This chapter illustrates these improvements to the response graphs as compared to the original model output as developed by Zhao and modified by MacDonald. Two hover cases, two 60 knot cases and a 140 knot case are presented.

The first case, figure 7-1, shows the response of the helicopter to a one inch right cyclic input while in a hover. The major improvement noted in this case is in the pitch rate response to the roll input. The flight test indicates a pitch down followed after two seconds by a pitch up. Although still not correct, the new output does show the initial nose down pitch rate, but then reverts to the nose up. After 4 seconds the model can not be expected to accurately follow the flight test because the pilot began recovery by lowering the collective. The collective input is not modeled in this system. It was the correction in the value of Δsp that is mostly responsible for this

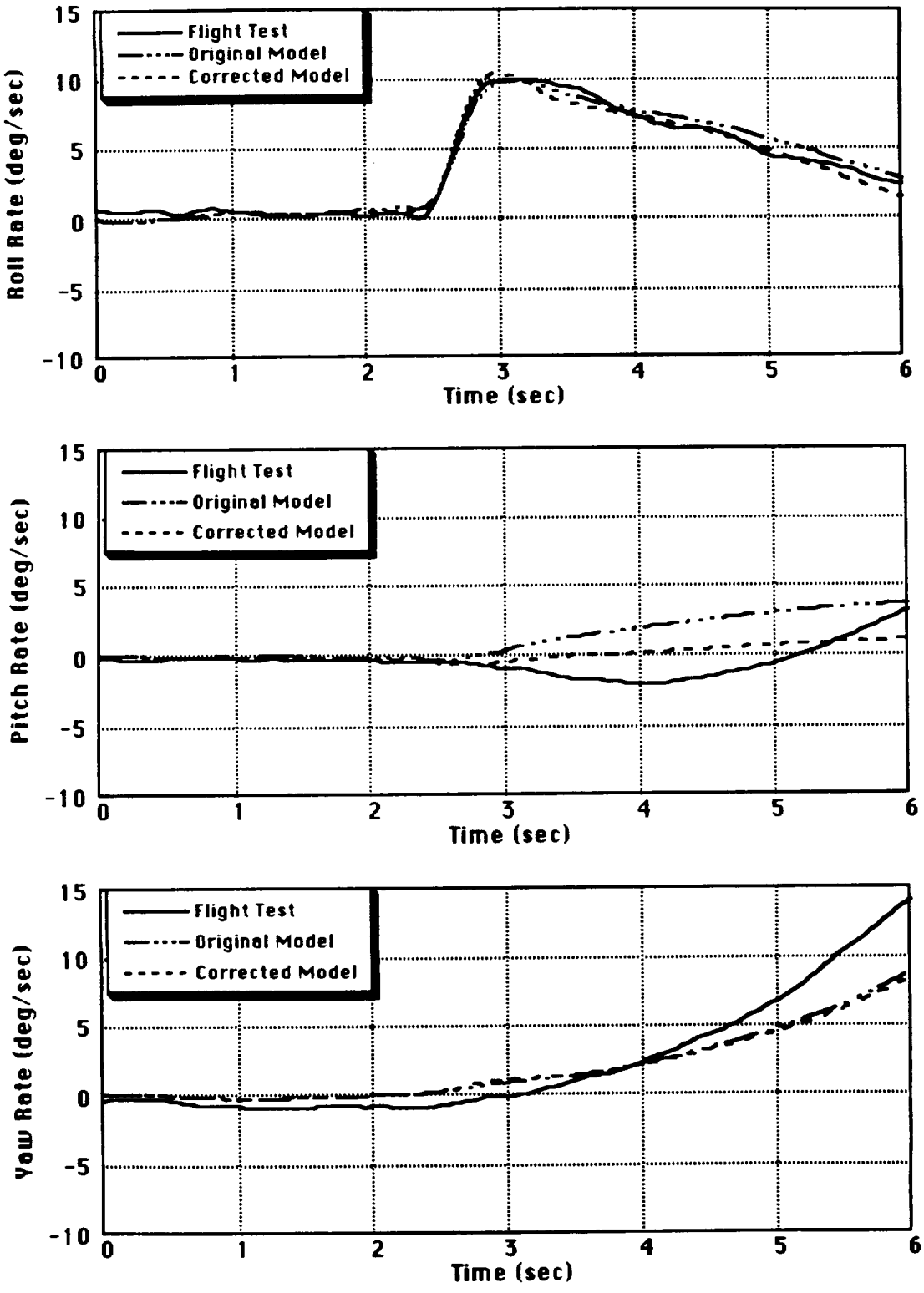

Figure 7-1: Response of the corrected full 27 state model, with dynamic inflow effects, to a 1" right cyclic input in a hover (AEFA Test 201).

improvement in pitch rate. Originally, with Δsp set at zero, the situation that was presented in figure 6-2 (a) was occurring; a right side down roll input was also causing a nose up pitching moment. As for the other angular rates, the roll response, which was very well correlated to flight test to start with, was improved slightly by the correction to twist, but the yaw response was basically unchanged.

The second hover case, figure 7-2, in which a one inch left pedal input is used, illustrates other kinds of changes. In this case the aim velocity for flight test was zero knots (hover). Maintaining a precise hover was difficult, however, for the pilots flying at over five thousand feet, and at the time of the test, the LASSIE system was indicating 14 knots forward airspeed. The original trim file indicated zero knots. It is this correction in velocity, plus some effect from the twist, that improved the roll rate response in lowering the peak and improving the roll acceleration (slope of the rate) after the peak. The velocity also caused the yaw rate response to show some indication of the bend at 3.8 seconds. Unfortunately, the pitch rate response shows even less correlation with flight test than it did previously. This points out the fact that the system is still not correctly modeling the effects of the downwash on the tail surfaces as the tail changes position due to the yaw. Another cause may be the control mixing since the left pedal input does affect B_{1s}. The values used in the mixing are linearizations of this nonlinear device, so inaccuracies may be present.

The first 60 knot case, shown in figure 7-3, demonstrates the response to a one inch left cyclic input. In addition to the other corrections discussed in this report, for this flight test case, errors in the velocity and gross weight were corrected. Overall there was not a significant change in the output. The pitch

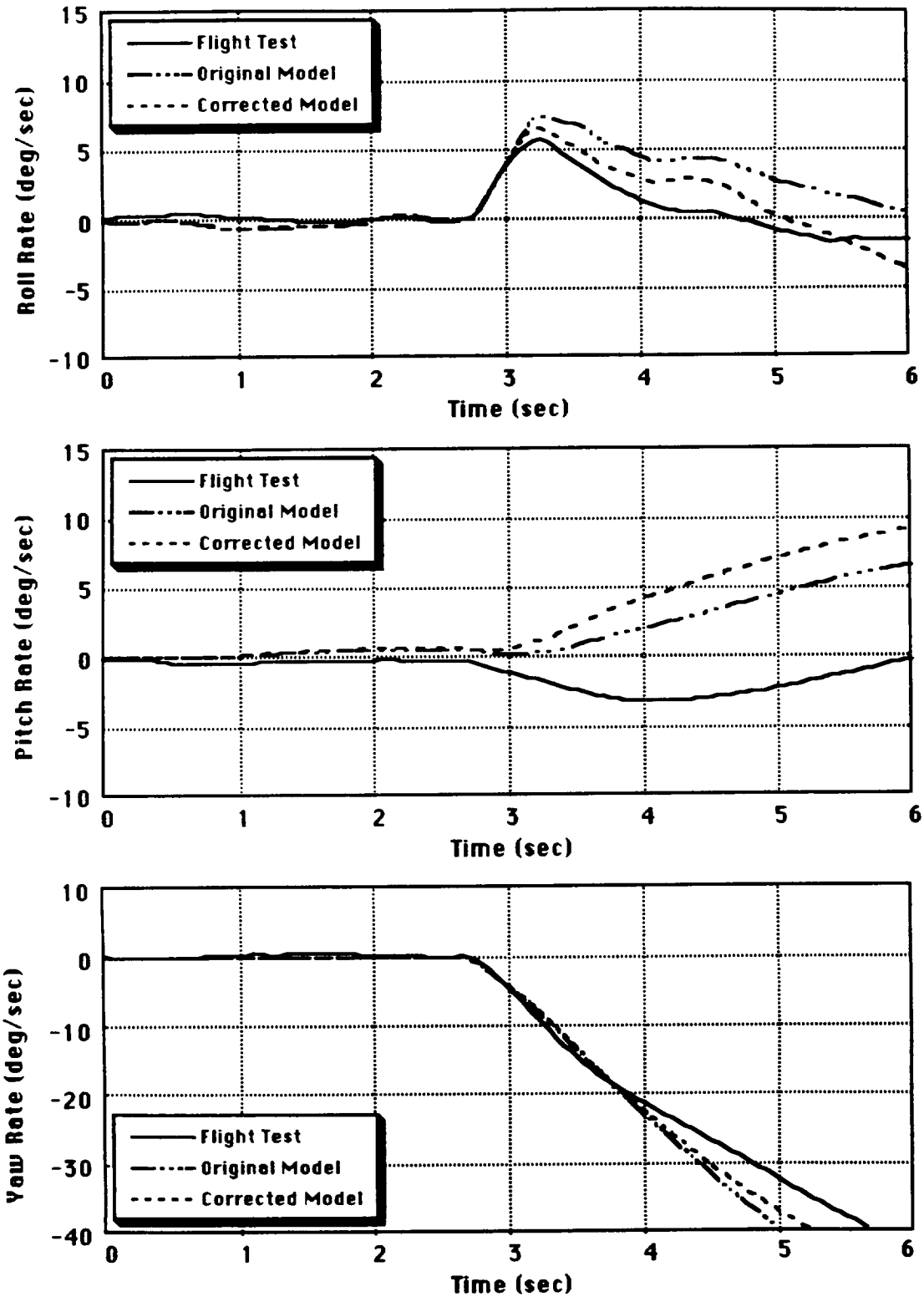

Figure 7-2: Response of the corrected full 27 state model, with dynamic inflow effects, to a 1" left pedal input in a hover (AEFA Test 209).

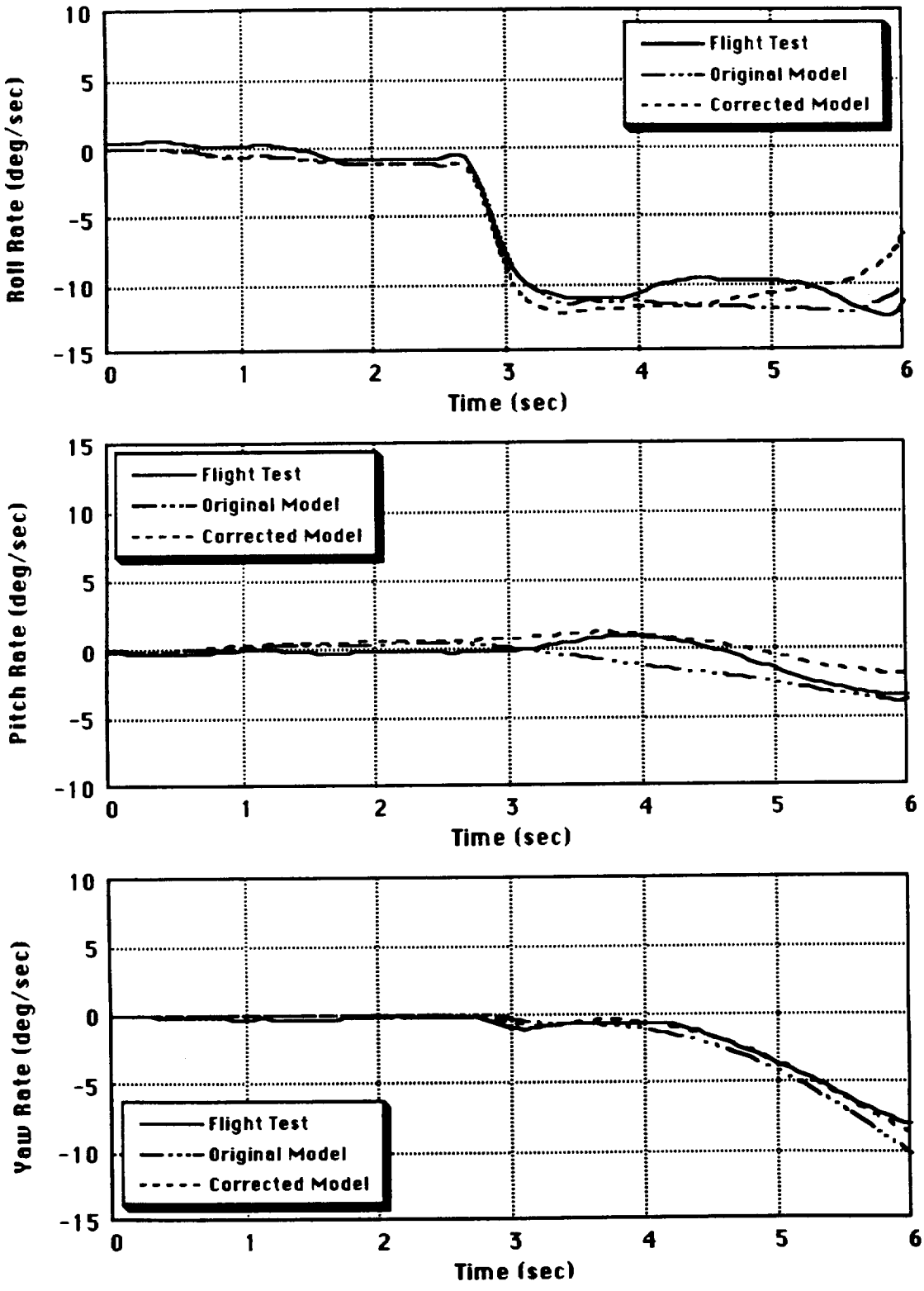

Figure 7-3: Response of the corrected full 27 state model, with dynamic inflow effects, to a 1" left cyclic input at 60 knots (AEFA Test 504).

does now show some of the tendency to pitch up before pitching down like the flight test. The yaw response is even closer to flight test than it was before.

The second 60 knot case, figure 7-4, shows a one half inch right pedal input. Like in the previous 60 knot case, the velocity had to be corrected, in addition to the overall corrections. The roll plot indicates a higher negative peak value than the original model, but then the acceleration is better after the peak. It should be noted that at 5 seconds, the pilot began a strong recovery due to the pitching rate, and the collective was used. The change in roll rate at 5.5 seconds is likely caused by the collective not being modeled. The model does show very good yaw-pitch coupling in this case as the pitch rate graph shows. The correction in both twist and velocity were responsible for the improvements. The on-axis response of the yaw rate shows much better improvement with the increased velocity and corrected twist along with the other changes.

The final case is at 140 knots with a half inch doublet pedal input, first to the left and then the right. Figure 7-5 shows the angular rates. This is a case where the corrections to the model had a generally negative effect on the correlation with flight test. The pitch rate response is slightly improved with a better pitch acceleration after the peak, but the peak is still too low. The off-axis response in roll rate is over-estimated, and the corrections to the program have tended to exacerbate that situation. The on-axis yaw response is only slightly changed.

These five cases demonstrate that the changes and corrections to the model and the trim input file did have a generally positive effect on the correlation of the model with flight test.

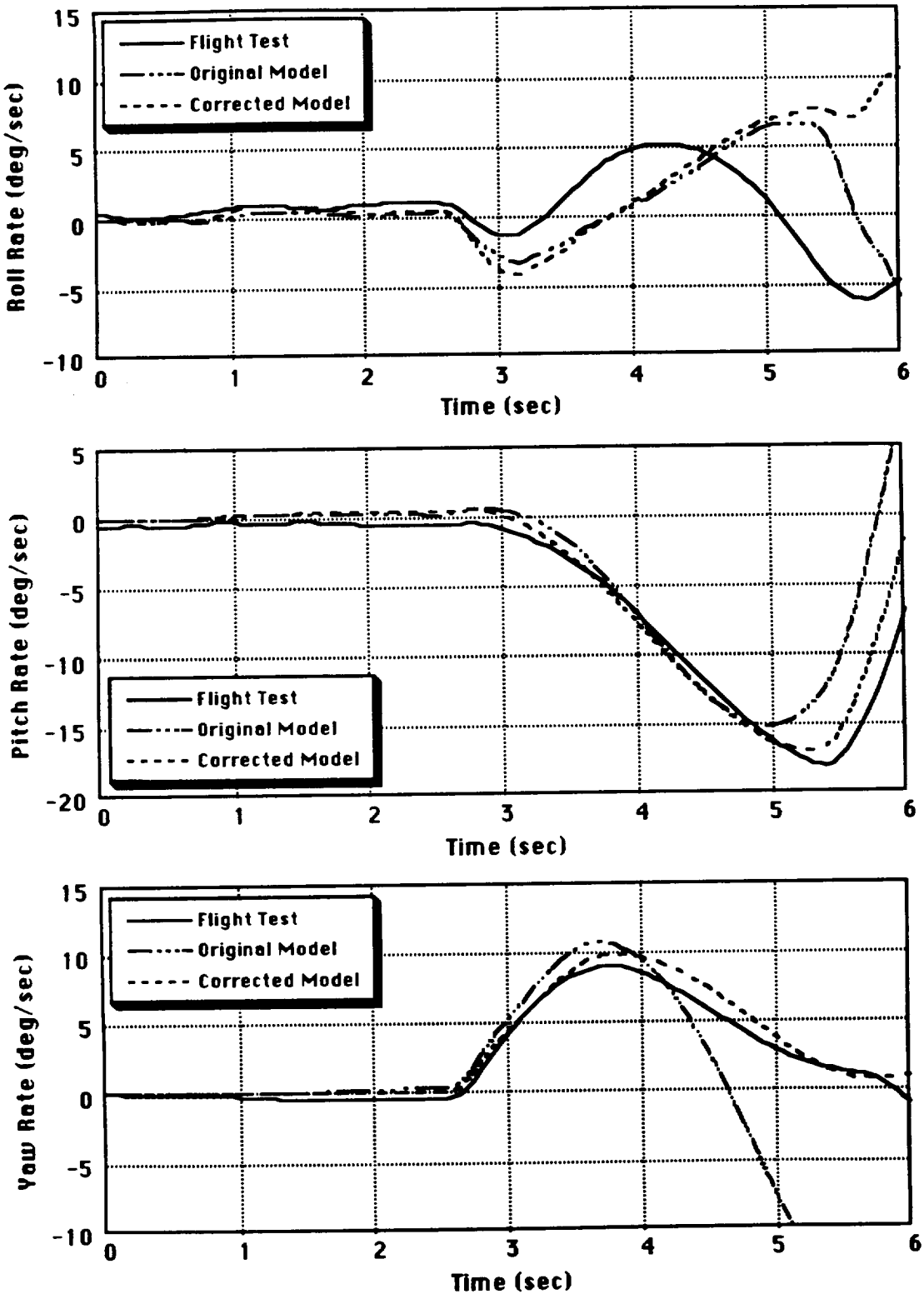

Figure 7-4: Response of the corrected full 27 state model, with dynamic inflow effects, to a 1/2" right pedal input at 60 knots (AEFA Test 502).

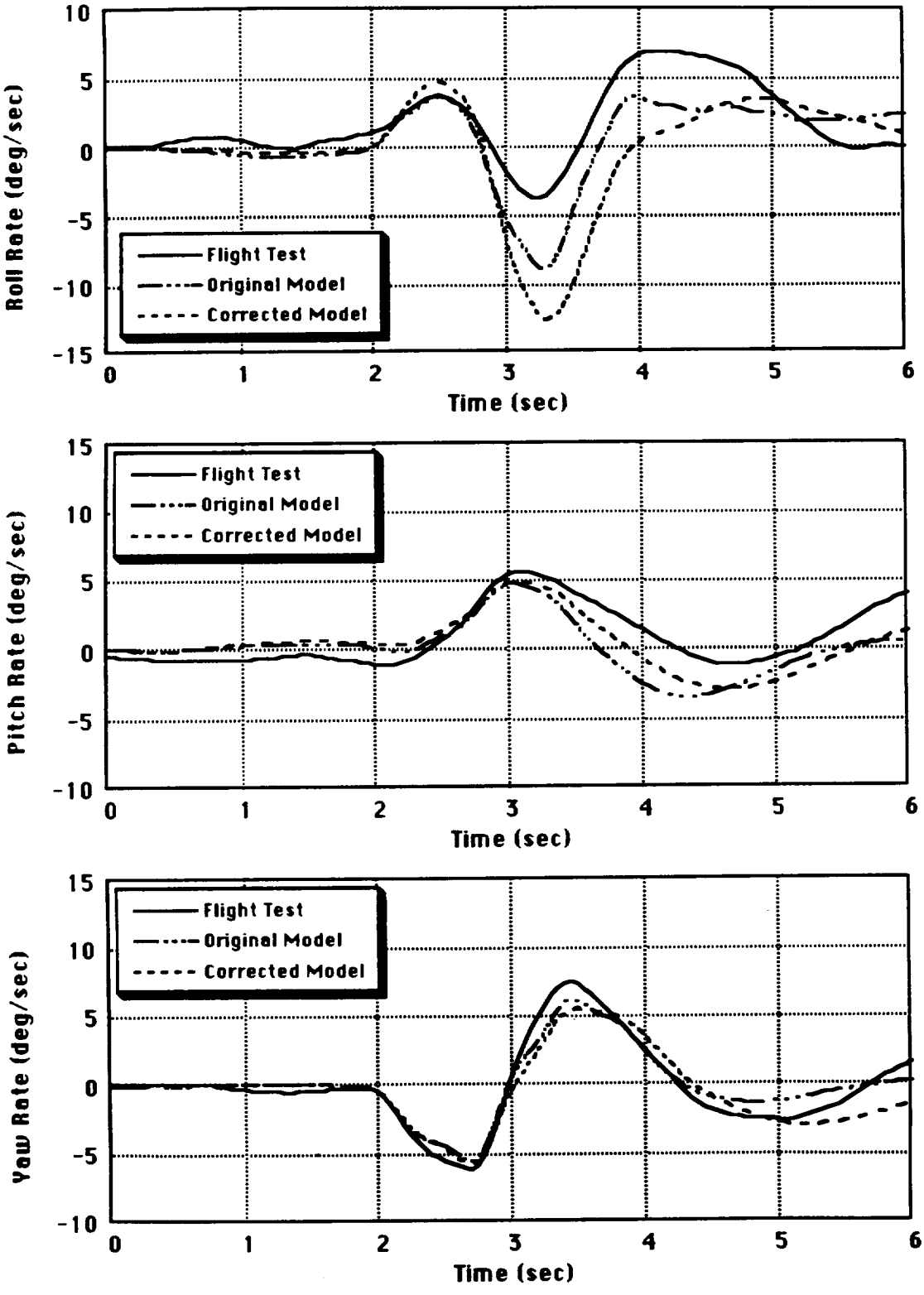

Figure 7-5: Response of the corrected full 27 state model, with dynamic inflow effects, to a 1/2" doublet pedal input at 140 knots (AEFA Test 309).

CHAPTER VIII

CONCLUSIONS AND RECOMMENDATIONS

An analytically linearized model of a helicopter, incorporating rotor blade dynamics and dynamic inflow, had been developed that promised advantages in stability and control analysis. This model has been examined with the goal of improving its capabilities for this type of analysis.

To this goal, integral details of the mathematical model and the validating flight test have been explored and documented. The computer implementation of the system has been substantially improved to increase speed, efficiency and ease of use. Several hidden modeling errors have been discovered and corrected. And finally, the use of the trim input file has been studied with numerous corrections to the values that have been used and corrections to how they are derived.

Although the correlation to flight test was not perfected, it was more the objective of this study to correct the fundamental problems in the system; both in the physics of the problem and in the modeling. Many of these types of problems were resolved. Future sensitivity analysis performed with this model can be done more confidently, in that the variations to the parameters will be due to the helicopter and not due a modeling error.

However, several areas still remain to be explored further. The entire area of the effect of the downwash on the tail still needs to be examined. Although the subject has been approached in past work, this study did not address it. Problems with off-axis coupling still remain and are probably due

to this complicated feature of the model. The off-line program to calculate these effects should be implemented into the model to provide these values automatically. Presently they must be input manually in the trim input file.

Although comparison with Black Hawk flight test has shown very good correlation, the model should also be correlated against other helicopter flight tests. A hingeless rotor helicopter would indicate the usefulness of the hub geometry flexibility that is built into the model.

In terms of implementation, one question remains. In order to export this model to other research organizations, it would be advantageous to operate the system from a desktop computer. Due to memory restrictions, however, the main program, "matrix", will have to be partitioned into several smaller clusters such as rotor aerodynamics, tail aerodynamics, fuselage aerodynamics, matrix development, etc. These smaller partitions could then be run individually with lower overall memory requirements.

Finally, the model is currently not easily extendable. Addition of collective input, drive train/engine dynamics, fuselage flexibility or blade torsion would be extremely difficult. It would be very valuable to re-derive the system using a modern symbolic program, such as Mathematica, to produce a new model that would be capable of these other modeling areas.

REFERENCES

[1] Zhao, X., "A Study of Helicopter Stability and Control Including Blade Dynamics," Ph.D. diss., Princeton University, 1988.

[2] Ellis, C.W., "Effects of Rotor Dynamics on Helicopter Automatic Control System Requirements," *Aeronautical Engineering Review* (July 1953).

[3] Hansen, R.S., "Toward a Better Understanding of Helicopter Stability Derivatives," *Journal of the American Helicopter Society* 29-2 (1984).

[4] Curtiss, H.C., Jr., "Stability and Control Modelling," Paper No. 41 in *Twelfth European Rotorcraft Forum,* September 1986.

[5] Hall, W.E., Jr. and A.E. Bryson, Jr., "Inclusion of Rotor Dynamics in Controller Design for Helicopters," *Journal of Aircraft* 10-4 (April 1974).

[6] Curtiss,H.C., Jr. and N.K. Shupe, "Stability and Control Theory for Hingeless Rotors," in *the Twenty Seventh Annual Forum of the American Helicopter Society,* May 1971.

[7] Gaonkar, G.H. and D.A. Peters, "Effectiveness of Current Dynamic-Inflow Models in Hover and Forward Flight," *Journal of the American Helicopter Society* 31-2 (1986).

[8] Chen, R.T.N. and W.S. Hindson, "Influence of Dynamic Inflow on the Helicopter Vertical Response," *Vertica* 11 (1987).

[9] Howlett, J.J., "UH-60A Black Hawk Engineering Simulation Program: Volume I - Mathematical Model," *NASA CR-166309,* 1981.

[10] Abbott, W.Y., J.O. Benson, R.G. Oliver, and R.A. Williams, "Validation Flight Test Of UH-60A for Rotorcraft Systems Integration Simulator (RSIS)," *USAAEFA PROJECT No. 79-24,* 1982.

[11] MacDonald, B.A., "Studies in Helicopter Dynamics Including System Identification Using a Linear Model of 20,000 lb Utility Helicopter," M.S.E. thesis, Princeton University, 1990.

[12] Gessow, A. and G.C. Myers, Jr., *Aerodynamics of the Helicopter*. College Park Press, 1985.

[13] Zhao, X. and H.C. Curtiss, Jr., "A Linearized Model of Helicopter Dynamics Including Correlation with Flight Test," in *The Second International Conference on Rotorcraft Basic Research,* Maryland, February 1988.

[14] Curtiss, H.C., Jr. and T.R. Quackenbush, "The Influence of the Rotor Wake on Rotorcraft Stability and Control," Paper No. 70 in *The Fifteenth European Rotorcraft Forum,* September 1989.

[15] Cooper, D.E., "YUH-60A Stability and Control," *The Journal of the American Helicopter Society* 23 (1978).

[16] Ballin, M.C., "Validation of a Real-Time Engineering Simulation of the UH-60A Helicopter," *NASA TM-88360,* 1987.

[17] Bailey, F.J., Jr., "A Simplified Theoretical Method of Determining the Characteristics of a Lifting Rotor in Forward Flight," *NACA Report 716,* 1941.

[18] Curtiss, H.C., Jr., Unpublished notes on the UH-60A Black Hawk Flight-Control System, 1989.

[19] Seckel, E. and H.C. Curtiss, Jr., "Rotor Contributions to Helicopter Stability Parameters," *Princeton University Department of Mechanical and Aerospace Engineering Report No. 659,* 1963